GALCIT FM 96-6

BLIMPK Simulations of Hypervelocity Boundary Layers - Boundary Layer Integral Matrix Procedure with Kinetics

Philippe H. Adam

Graduate Aeronautical Laboratories
California Institute of Technology
Pasadena, California 91125

GALCIT Report FM 96-6

August 1996

Contents

Nomenclature

Symbols

C - Chapman-Rubesin parameter
$\overline{C}_p$ - frozen specific heat of gas mixture
C_{p_i} - specific heat of species i
$\overline{D}$ - reference binary diffusion coefficient
D_i^T - multicomponent thermal diffusion coefficient for species i
$\mathcal{D}_{ij}$ - binary diffusion coefficient for species i and j
f - stream function
h - static enthalpy of gas
h_i - static enthalpy of molecular species i
h_i^o - heat of formation
H_T - total enthalpy
j_i - diffusional mass flux of species i per unit area away from the surface
K_i - mass fraction of molecular species i
$\tilde{K}_k$ - mass fraction of element k
L - reference length
M - Mach number
$\mathcal{M}_i$ - molecular weight of species i
$\dot{m}$ - mass flux
p - pressure
q_a - diffusional heat flux away from the surface
q_r - one-dimensional radiant heat flux to the surface
r - distance normal to body
Re - Reynolds number
s - distance along body from stagnation point
Sc_t - turbulent Schmidt number
St - Stanton number
T - static temperature
u - velocity component parallel to body
v - velocity component normal to body
v_s - shock speed
x - distance from tip

x_i - mole fraction of molecular species i
y - distance normal to body from surface

α_{ki} - mass fraction of element k in species i
β - streamwise pressure gradient parameter
Δ - streamwise distance between nodes
ϵ - emissivity
η - transformed transverse coordinate
ν - kinematic viscosity
ξ - transformed streamwise coordinate
ρ - density
$\rho\varepsilon_D$ - turbulent eddy diffusivity
$\rho\varepsilon_H$ - turbulent eddy conductivity
$\rho\varepsilon_M$ - turbulent eddy viscosity
σ - Stefan-Boltzmann constant
Θ - body angle
ψ_i - rate of mass generation of species i per unit volume due to chemical reactions

Subscripts

c - cone
e - edge
i - ith species or ith nodal point
ℓ - streamwise index
w - wall
0 - stagnation condition
1 - reference condition (boundary layer edge, for example)

Superscripts

κ - parameter equal to 1 for axisymmetric flows and 0 for two-dimensional flows
$*$ - nondimensionalized quantity

Chapter 1

Introduction

When designing reentry spacecraft, whether for Earth reentry or for other planetary atmospheres, it is important to obtain an accurate measure of surface heating rates throughout the pertinent reentry trajectory. Heat transfer, on internal and external surfaces, largely dictates the shielding method and material to be used. For this reason, simulating the flowfield around the vehicle is quite important, in particular when it comes to simulating the viscous flowfield at the boundary layer level, close to the surface. At reentry speeds on the order of several kilometers per second, the flow is known to dissociate inside the hot boundary layer and gas-phase as well as surface reactions including ablation must be accounted for.

During the design of the space shuttle, for example, in order to the select the best Thermal Protection System (TPS) possible, studies had to be carried out to look at reaction rate and surface catalycity effects on the heat transfer rate. Furthermore, this had to be done quickly for several possible vehicle configurations. Therefore, the need for a fast but flexible boundary layer code led to the development of BLIMP, a Boundary Layer Integral Matrix Procedure satisfying these requirements. At the time, fast meant that a solution had to be obtained with a minimal number of grid points. Flexible meant it had to be easy to try different chemical models, i.e. different species compositions, ablation models and boundary layer reactions.

Continuously updated since, the latest version of BLIMP was renamed BLIMPK because of the addition of kinetics as an option. The code is therefore capable of simulating multicomponent boundary layers with frozen, equilibrium or nonequilibrium chemistry. Unequal concentration and thermal diffusion are other options and laminar flows as well as turbulent flows (with built-in eddy viscosity models) can be computed. Gas phase reactions and surface reactions are parameters and a maximum of 15 transverse nodal points is all that is needed to capture the profile of the boundary layer. The number of possible streamwise nodes is unlimited.

A detailed description of the main program and the numerical scheme is available in Bartlett and Kendall [1967] for the first version of BLIMP including solely equilibrium chemistry. The nonequilibrium chemistry extension including surface reactions is discussed in Tong *et.al.* [1973] and the various turbulence models are compared in Evans [1975]. A brief input guide for the latest version of BLIMPK, called BLIMP88, can be found in Murray [1988]. The present report will only attempt to summarize the important ideas contained in the original reports relevant to understanding and running the code. Examples of T5 generated flows computed with BLIMP88 are also included. In particular, different simulations of an axisymmetric hypervelocity boundary layer on a sharp cone will be considered.

Chapter 2

Conservation Equations

The equations of mass, momentum, energy and species conservation for a multicomponent chemically reacting boundary layer are derived and discussed in Dorrance [1962] and Anderson [1989]. The coordinate system used is depicted below in Figure 2.1. s is defined as the coordinate along the body from the stagnation point, y as the coordinate normal to the body and r as the local radius in the boundary layer in the meridional plane.

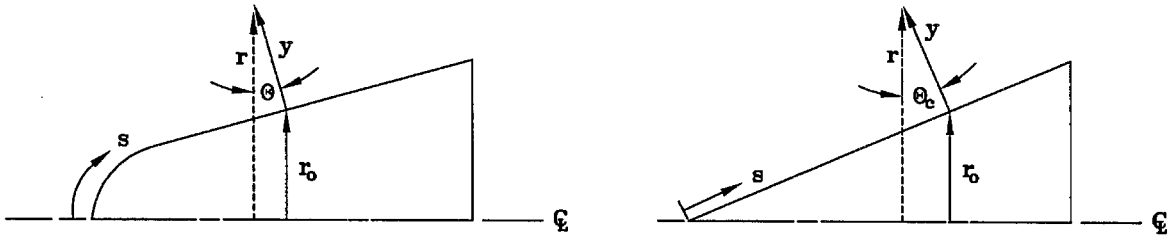

Figure 2.1 - Coordinate System

Mass conservation

$$\frac{\partial}{\partial s}(\rho u r^{\kappa}) + \frac{\partial}{\partial y}(\rho v r^{\kappa}) = 0 \tag{2.1}$$

where κ equals 1 for axisymmetric flows and 0 for two-dimensional flows. The velocity components parallel and normal to the body are u and v respectively. ρ is the density.

Momentum conservation

$$\rho u \frac{\partial u}{\partial s} + \rho v \frac{\partial u}{\partial y} = \frac{1}{r^{\kappa}} \frac{\partial}{\partial y}\left[\rho r^{\kappa}(\nu + \varepsilon_M)\frac{\partial u}{\partial y}\right] - \frac{\partial p}{\partial s} \tag{2.2}$$

where ν is the kinematic viscosity, ε_M the turbulent eddy viscosity, and p the pressure.

Energy conservation

$$\rho u\frac{\partial H_T}{\partial s} + \rho v\frac{\partial H_T}{\partial y} = \frac{1}{r^\kappa}\frac{\partial}{\partial y}\left[\rho r^\kappa(\nu + \varepsilon_M)\frac{\partial(u^2/2)}{\partial y} + r^\kappa(\lambda + \rho\varepsilon_H\overline{C}_p)\frac{\partial T}{\partial y}\right.$$
$$+ r^\kappa\sum_i\left(\rho\varepsilon_D\frac{\partial K_i}{\partial y} - j_i\right)h_i$$
$$\left. - \frac{r^\kappa RT}{\rho}\sum_i\sum_j\frac{x_jD_i^T}{\mathcal{M}_i\mathcal{D}_{ij}}\left(\frac{j_i}{K_i} - \frac{j_j}{K_j}\right) + r^\kappa q_r\right] \tag{2.3}$$

where, by definition, the total enthalpy $H_T = h + \frac{u^2}{2}$ with $h = \sum_i K_i h_i$ and $h_i = \int_{T^0}^{T} C_{p_i}dT + h_i^0$. λ is the thermal conductivity, ε_H the turbulent eddy conductivity and ε_D the turbulent eddy diffusivity. The mass fraction and mole fraction of the i^{th} species are denoted by K_i and x_i respectively and the diffusional mass flux of that species by j_i. D_i^T is the corresponding multicomponent thermal diffusion coefficient and $\mathcal{D}_{ij}$ the multicomponent binary diffusion coefficient. The one-dimensional net radiant heat flux to the surface due to absorption and emission is q_r.

Species conservation

$$\rho u\frac{\partial K_i}{\partial s} + \rho v\frac{\partial K_i}{\partial y} = \frac{1}{r^\kappa}\frac{\partial}{\partial y}\left[r^\kappa\left(\rho\varepsilon_{D_i}\frac{\partial K_i}{\partial y} - j_i\right)\right] + \psi_i \tag{2.4}$$

where ψ_i denotes the rate of mass generation of species i due to chemical reactions.

The diffusional mass flux j_i can be obtained explicitly by approximating the binary diffusion coefficient $\mathcal{D}_{ij}$ by the function $\mathcal{D}_{ij} \approx \frac{\overline{D}(T,P)}{F_iF_j}$, where $\overline{D}$ is a reference diffusion coefficient and F_i is a diffusion factor for species i, and thereafter solving the Stefan-Maxwell equation

$$\frac{\partial x_i}{\partial y} = \sum_j\frac{x_ix_j}{\rho\mathcal{D}_{ij}}\left[\frac{j_j + D_j^T\frac{\partial \ln T}{\partial y}}{K_j} - \frac{j_i + D_i^T\frac{\partial \ln T}{\partial y}}{K_i}\right] \tag{2.5}$$

The resulting expression for j_i is given by

$$j_i = -\frac{\rho\overline{D}\mu_2}{\mu_1\mathcal{M}}\left[\frac{\partial Z_i}{\partial y} + (Z_i - K_i)\frac{\partial \mu_4}{\partial y}\right] \tag{2.6}$$

defining

$$Z_i \equiv \frac{\mathcal{M}_ix_i}{F_i\mu_2}$$

$$\mu_1 \equiv \sum_j x_jF_j \qquad \mu_2 \equiv \sum_j\frac{\mathcal{M}_jx_j}{F_j} \qquad \mu_3 \equiv \sum_i\frac{Z_i}{\mathcal{M}_i} \qquad \mu_4 \equiv \ln(\mu_2T^{c_t})$$

$$c_t \approx -0.5$$

$$\tilde{C}_p \equiv \sum_i Z_i C_{p_i}$$

$$\tilde{h} \equiv \sum_i Z_i h_i \tag{2.7}$$

Details on this bifurcation approximation and the derivation of the coefficients listed in (2.7) can be found in Tong *et.al.* [1973].

The diffusional heat flux away from the surface can be expressed with the help of (2.7) as

$$q_a = -\left\{\rho(\varepsilon_M + \nu)\frac{\partial\left(\frac{u^2}{2}\right)}{\partial y} + (\lambda + \rho\varepsilon_H\overline{C}_p)\frac{\partial T}{\partial y} + \rho\varepsilon_D\left(\frac{\partial h}{\partial y} - \overline{C}_p\frac{\partial T}{\partial y}\right)\right.$$
$$\left. + \frac{\rho\overline{D}\mu_2}{\mu_1\mathcal{M}}\left[\frac{\partial\tilde{h}}{\partial y} - \left(\tilde{C}_p + \frac{c_t^2 R}{\mu_1\mu_2}\right)\frac{\partial T}{\partial y} + c_t RT\frac{\partial\mu_3}{\partial y} + (\tilde{h} - h + c_t RT\mu_3)\frac{\partial\mu_4}{\partial y}\right]\right\} \tag{2.8}$$

For computational reasons outlined in Bartlett and Kendall [1967], it is often preferable to rewrite the conservation equations by introducing "elemental" mass fractions rather than "species" mass fractions. In the case of equilibrium chemistry, for example, this effectively reduces the size of the matrix to be inverted in the solution procedure for the system of differential equations describing the problem. Therefore, defining the elemental mass fraction for an element k as

$$\tilde{K}_k = \sum_i \alpha_{ki} K_i \tag{2.9}$$

and

$$\tilde{Z}_k \equiv \sum_i \alpha_{ki} Z_i$$

$$\phi_k \equiv \sum_i \alpha_{ki}\psi_i \tag{2.10}$$

allows the diffusional mass flux to be rewritten as

$$j_k = -\frac{\rho\overline{D}\mu_2}{\mu_1\mathcal{M}}\left[\frac{\partial\tilde{Z}_k}{\partial y} + \left(\tilde{Z}_k - \tilde{K}_k\right)\frac{\partial\mu_4}{\partial y}\right] \tag{2.11}$$

The new equations of conservation of mass, momentum, energy and "elemental" species then become

$$\frac{\partial}{\partial s}(\rho u r^\kappa) + \frac{\partial}{\partial y}(\rho v r^\kappa) = 0 \tag{2.12}$$

$$\rho u\frac{\partial u}{\partial s} + \rho v\frac{\partial u}{\partial y} = \frac{1}{r^\kappa}\frac{\partial}{\partial y}\left[\rho r^\kappa(\nu + \varepsilon_M)\frac{\partial u}{\partial y}\right] - \frac{\partial p}{\partial s} \tag{2.13}$$

$$\rho u \frac{\partial H_T}{\partial s} + \rho v \frac{\partial H_T}{\partial y} = \frac{1}{r^\kappa} \frac{\partial}{\partial y} [r^\kappa (-q_a + q_r)] \tag{2.14}$$

$$\rho u \frac{\partial \tilde{K}_k}{\partial s} + \rho v \frac{\partial \tilde{K}_k}{\partial y} = \frac{1}{r^\kappa} \frac{\partial}{\partial y} \left[r^\kappa \left(\rho \varepsilon_{D_k} \frac{\partial \tilde{K}_k}{\partial y} - j_k \right) \right] + \phi_k \tag{2.15}$$

where, by definition, $\phi_k \equiv \sum_i \alpha_{ki} \psi_i$.

In the case of equilibrium chemistry $\phi_k = 0$ since there is no production whereas for nonequilibrium chemistry

$$\begin{aligned} \alpha_{ki} &= 0 , \quad k \neq i \\ \alpha_{ki} &= 1 , \quad k = i \end{aligned} \tag{2.16}$$

Finally, to complete the formulation of the problem, expressions for the equation of state and the transport properties must be provided. This is taken care of within BLIMPK with standard mixture formulas for viscosity (Buddenberg-Wilke) and thermal conductivity (Mason-Saxena), taking into account the exact composition of the gas at the points of interest. Also needed are the equilibrium or nonequilibrium relations. Tables A.1 and A.2 in Appendix A summarize the more important reactions for flows involving air and carbon dioxide respectively (Chen *et.al.* [1993], Park *et.al.* [1994]).

As far as closure for the turbulence parameters, BLIMPK relys on different mixing length correlations, the boundary layer being generally split into a wall region and a wake region. Details can be found in Evans [1975] where the more successful of the three models included in BLIMPK seems to be the one derived by Cebeci and Smith which accounts for a variable turbulent Prandtl number. The other two models are attributed to Kendall and to Bushnell. The user must specify the station along the body where the code is to switch from fully laminar to fully turbulent. This can also be accomplished by specifying a momentum thickness beyond which the switch is to take place. BLIMPK accounts for a buffer-transition zone between the last laminar station and the first turbulent one. This manifests itself by a slight overshoot in the initial turbulent heat transfer.

It should be noted that, the set of conservation equations (2.12)-(2.15) being parabolic, boundary conditions necessary for the solution of the problem must include specifying variables and derivatives at the edges of the computational domain and at the initial "time". In the case of a boundary layer, this translates to specifying variables and derivatives at the surface of the geometric model being considered, at the edge of the boundary layer and at the initial nodal point where the solution proceeds from. Different boundary conditions will be discussed in the following section.

Chapter 3

Coordinate Transformation

Once all equations needed to close the problem have been identified - conservation of mass, momentum, energy and species or elements, state, viscosity, conductivity, chemistry and mixing length - one can go on to solve the problem by appropriately discretizing them. It is however quite often in the interest of speed, accuracy and simplicity to transform these equations from the original (s,y) coordinate system to a different system. In the case of the compressible boundary layer equations under arbitrary boundary conditions, one usually resorts to one form or another of the standard Levy-Lees transformation (Lees [1956]).

The Levy-Lees transformation from the (s,y) coordinate system to (ξ,η) is given by the following pair of equations

$$\begin{aligned} \xi &= \int_o^s \rho_1 u_1 \mu_1 r_o^{2\kappa} ds \\ \eta &= \frac{r_o^{\kappa} u_1}{\sqrt{2\xi}} \int_o^y \rho dy \end{aligned} \tag{3.1}$$

An implicitly determined stretching parameter $\alpha_H(\xi)$ is added within the BLIMPK formulation to keep the thickness of the boundary layer constant in the $\overline{\eta}$ direction as the solution marches in the ξ direction. The new set of coordinates $(\overline{\xi},\overline{\eta})$ is therefore given by

$$\begin{aligned} \overline{\xi} &= \xi \\ \overline{\eta} &= \frac{\eta}{\alpha_H} \end{aligned} \tag{3.2}$$

The additional equation now required by the introduction of the new parameter α_H is obtained by fixing the u component of velocity to c at a given $\overline{\eta}_c$ node, i.e.

$$f'\Big|_{\overline{\eta}_c} = c f'\Big|_{\overline{\eta}_{edge}} \tag{3.3}$$

where f is the stream function given by

$$f - f_w = \int_0^\eta \frac{u}{u_1} d\eta = \alpha_H \int_0^{\overline{\eta}} \frac{u}{u_1} d\overline{\eta} \tag{3.4}$$

and, by definition,

$$f' = \frac{\partial f}{\partial \overline{\eta}} = \alpha_H \frac{u}{u_1} \tag{3.5}$$

Finally, if one takes r to be a function of y, as would be the case for thin axisymmetric bodies where the boundary layer thickness δ is comparable to the body radius r_o, the $(\overline{\xi}, \overline{\eta})$ system can be transformed to a $(\hat{\xi},\hat{\eta})$ system such that

$$\begin{aligned} \hat{\xi} &= \int_0^s \rho_1 u_1 \mu_1 r_o^{2\kappa} ds \\ \hat{\eta} &= \frac{u_1}{\alpha_H \sqrt{2\hat{\xi}}} \int_0^y \rho r^\kappa dy \end{aligned} \tag{3.6}$$

with now, dropping the hats,

$$\begin{aligned} f - f_w &= \alpha_H \int_0^\eta \frac{u}{u_1} d\eta \\ f_w &= -\frac{1}{\sqrt{2\xi}} \int_0^\xi \frac{\rho_w v_w}{\rho_1 u_1 \mu_1 r_o^\kappa} d\xi \end{aligned} \tag{3.7}$$

Since the (s,y) derivatives can now be rewritten in terms of (ξ,η) derivatives using

$$\begin{aligned} \left.\frac{\partial}{\partial s}\right|_y &= \left.\frac{\partial}{\partial \xi}\right|_\eta \left.\frac{\partial \xi}{\partial s}\right|_y + \left.\frac{\partial}{\partial \eta}\right|_\xi \left.\frac{\partial \eta}{\partial s}\right|_y \\ \left.\frac{\partial}{\partial y}\right|_s &= \left.\frac{\partial}{\partial \xi}\right|_\eta \left.\frac{\partial \xi}{\partial y}\right|_s + \left.\frac{\partial}{\partial \eta}\right|_\xi \left.\frac{\partial \eta}{\partial y}\right|_s \end{aligned} \tag{3.8}$$

the transformed equations for conservation of momentum, energy and elements become

$$f f'' + \left[\frac{C\left(1 + \frac{\varepsilon_M}{\nu}\right)}{\alpha_H} f''\right]' + \beta\left(\alpha_H^2 \frac{\rho_1}{\rho} - f'^2\right) = 2\left(f' \frac{\partial f'}{\partial \ln \xi} - f'^2 \frac{\partial \ln \alpha_H}{\partial \ln \xi} - f'' \frac{\partial f}{\partial \ln \xi}\right) \tag{3.9}$$

$$f H_T' + \left(-q_a^* + q_r^*\right)' = 2\left(f' \frac{\partial H_T}{\partial \ln \xi} - H_T' \frac{\partial f}{\partial \ln \xi}\right) \tag{3.10}$$

$$f \tilde{K}_k' + \left(\frac{\tilde{\varepsilon}_M}{\alpha_H Sc_t} \tilde{K}_k' - j_k^*\right)' + \left(\frac{\phi_k}{\rho}\right)\left(\frac{\rho_e \mu_e \alpha_H}{\alpha^{*2}}\right) = 2\left(f' \frac{\partial \tilde{K}_k'}{\partial \ln \xi} - \tilde{K}_k' \frac{\partial f}{\partial \ln \xi}\right) \tag{3.11}$$

assuming $p = p(\xi)$ only and where the $(\,)^*$ refers to quantities that have been appropriately nondimensionalized. The streamwise pressure gradient parameter β and the Chapman-Rubesin parameter C are respectively defined as

$$\beta \equiv 2\frac{\partial \ln u_1}{\partial \ln \xi} \tag{3.12}$$

$$C \equiv \frac{\rho\mu}{\rho_1\mu_1} \tag{3.13}$$

It should be noted that after the coordinate transformation, the equation of mass conservation is identically satisfied. Furthermore, an interesting consequence of similarity is that along with vanishing β, the right hand side of all the equations listed above vanish as well. The system is therefore reduced to a system of ordinary differential equations! Details of every step in the derivation of these transformed equations can be found in Bartlett and Kendall [1967].

Typical boundary conditions for this formulation consist in specifying at the edge of the boundary layer the velocity, enthalpy and elements given as $f'_e = \alpha_H$, H_{T_e} and $\tilde{K}'_{k_e}$ respectively as well as, for example, the edge pressure, entropy, or mass fractions. At the wall, the corresponding conditions could also include $H_{T_w} = h_w(\xi)$ and $\tilde{K}'_{k_w}(\xi)$ along with the no slip condition $f'_w = 0$. Many other possible wall boundary conditions are listed in Tong *et.al.*[1973] and are detailed in the actual BLIMPK input guide in the Appendix of Murray [1988].

Chapter 4

Discretization and Integral Matrix Procedure

The first step in implementing the integral matrix procedure is determining the size of the grid to be used, in particular the number of nodal points to be considered across the boundary layer (η - direction) and along the body (ξ - direction). The number of ξ points and the spacing in between depends on the geometry and the edge properties, since a converged solution, as will be shown in this section, is output for each one of these streamwise stations once the equations have been solved across the boundary layer strip. In the case of a boundary layer on an axisymmetric body with constant edge conditions, for example, one would only need to pick enough points to resolve the geometry. A blunt body would require a dense grid near the nose to account for the rapidly changing flow conditions but further downstream, the grid could be less refined. If the flow were similar, as in the case of a zero pressure gradient boundary layer, refinement would be useless since no matter what station one looked at, the profiles would be identical.

It is really the number of η points that is the controlling factor as far as how fast and accurate a solution can be obtained. Furthermore, it is the main idea behind the integral matrix procedure to minimize the number of transverse nodes needed to obtain an accurate solution. This is achieved by spline fitting the primary dependent variables - f, H_T and $\tilde{K}_k$ - and their derivatives with respect to η in between these nodes with Taylor series. Examples with as little as seven points across the boundary are shown in Bartlett and Kendall [1967] to be accurate to several significant figures and ones with eleven points across the boundary layer to be almost indistinguishable from the exact solution. The maximum number of η points allowed by BLIMPK is accordingly 15 and the code allows the user to redistribute the nodes at different ξ stations to account for varying streamwise conditions such as transition to turbulence, blowing, suction, etc. which might strongly affect the overall shape of the boundary layer.

4.1 η Discretization

Assuming the boundary layer is resolved by N points at distances η_i and that $p(\eta)$ is one of the primary variables - f, H_T, $\tilde{K}_k$ - continuous along with its derivatives around $\eta = \eta_i$, one can write its Taylor series expansion as

$$p_{i+1} = p_i + p_i'\delta\eta + p_i''\frac{\delta\eta^2}{2!} + p_i'''\frac{\delta\eta^3}{3!} + p_i^{iv}\frac{\delta\eta^4}{4!} + \ldots \tag{4.1}$$

where

$$\delta\eta = \eta_{i+1} - \eta_i \tag{4.2}$$

A quick glance at equations (3.9)-(3.11) reveals that the highest derivatives to appear are f_i''', H_{T_i}'' and $\tilde{K}_{k_i}''$ so that one could truncate the series at the next highest derivative and assume it remains constant between η_i and η_{i+1}. The resulting set of linear equations for the primary dependent variables and their derivatives is therefore

$$-f_{i+1} + f_i + f_i'\delta\eta + f_i''\frac{\delta\eta^2}{2} + f_i'''\frac{\delta\eta^3}{8} + f_{i+1}'''\frac{\delta\eta^3}{24} = 0 \tag{4.3}$$

$$-p_{i+1} + p_i + p_i'\delta\eta + p_i''\frac{\delta\eta^2}{3} + p_{i+1}''\frac{\delta\eta^2}{6} = 0 \tag{4.4}$$

$$-p_{i+1}' + p_i' + p_i''\frac{\delta\eta}{2} + p_{i+1}''\frac{\delta\eta}{2} = 0 \tag{4.5}$$

where f_i', H_{T_i} and $\tilde{K}_{k_i}$ for all k elements are substituted for p_i. It should be noted that $f_i' = \alpha_H\frac{u}{u_1}$ is used instead of f since it is the actual velocity profile and not the stream function that is of interest. The total number of equations , when written for each set of nodes is (N-1)[5+2(k-1)] and the number of unknowns - f_n, f_n', f_n'', f_n''', α_H, H_{T_n}, H_{T_n}', H_{T_n}'', $\tilde{K}_{k_n}$, $\tilde{K}_{k_n}'$, $\tilde{K}_{k_n}''$ - comes up to N(4+3k)+1. The remaining equations come from the actual physical differential equations as well as the specific boundary conditions and the variables being only functions of $\delta\eta$, the system needs to be solved only once per strip, i.e. the matrix of coefficients need be inverted but once.

4.2 ξ Discretization

In the ξ direction standard finite difference expressions are used to discretize the derivatives that appear on the right hand side of equations (3.9)-(3.11). It should be noted again that if the solutions were similar, this step would not be necessary since the right hand side would vanish. Two- and three-point difference formulas are found to be sufficient (Bartlett and Kendall [1967]). This gives

$$2\left[\frac{d()}{d(\ln\xi)}\right]_\ell = d_o()_\ell + d_1()_{\ell-1} + d_2()_{\ell-2} \tag{4.6}$$

where the subscript ℓ refers to the ℓ^{th} streamwise position and where, for a two-point difference formulation,

$$d_o = \frac{2}{\ell\Delta_{\ell-1}}, \quad d_1 = -\frac{2}{\ell\Delta_{\ell-1}}, \quad d_2 = 0 \tag{4.7}$$

and for a three-point difference formulation,

$$d_o = 2\frac{{}_{\ell}\Delta_{\ell-1} + {}_{\ell}\Delta_{\ell-2}}{{}_{\ell}\Delta_{\ell-1}\,{}_{\ell}\Delta_{\ell-2}}, \quad d_1 = -2\frac{{}_{\ell}\Delta_{\ell-2}}{{}_{\ell}\Delta_{\ell-1}\,{}_{\ell-1}\Delta_{\ell-2}}, \quad d_2 = 2\frac{{}_{\ell}\Delta_{\ell-1}}{{}_{\ell}\Delta_{\ell-2}\,{}_{\ell-1}\Delta_{\ell-2}} \tag{4.8}$$

with

$${}_{\ell}\Delta_{\ell-1} = \ln\xi_{\ell} - \ln\xi_{\ell-1} = \ln\left(\frac{\xi_{\ell}}{\xi_{\ell-1}}\right) \tag{4.9}$$

Choosing either formulation is left up to the BLIMPK user as an option in the input file since it may depend on the particular problem being solved. However, it should be noted that for most problems, streamwise changes are very smooth and a the two-point expression is usually sufficient.

4.3 Solution Procedure

At this point, one could solve the linear Taylor series listed above along with the boundary layer equations, boundary conditions and, finally, the equation defining α_H to close the problem. However, this is not very practical since the boundary layer equations are not linear and therefore as simple to solve for the primary variables. In particular, the terms involving derivatives in η in the energy and element equations need to be simplified. The problem therefore reduces to one of linearizing these equations so that the system describing the entire problem is linear. To achieve this, the boundary layer equations must be integrated across the transverse η strips. This is equivalent to applying a square wave weighting function on top of the boundary layer taking on the value of unity between η_i and η_{i+1} and vanishing everywhere else.

The momentum equation (3.9) would therefore give, as an example,

$$\begin{aligned}
\int_{i-1}^{i} ff''d\eta \;+\; &\left[\frac{(C+\tilde{\varepsilon}_M)}{\alpha_H}f''\right]_{i-1}^{i} + \beta\alpha_H^2\int_{i-1}^{i}\frac{\rho_1}{\rho}d\eta - \beta\int_{i-1}^{i}f'^2d\eta \\
&= \int_{i-1}^{i} f'(d_o f' + d_1 f'_{\ell-1} + d_2 f'_{\ell-2})d\eta - \int_{i-1}^{i} f'^2\,[d_o\ln\alpha_H \\
&+ d_1(\ln\alpha_H)_{\ell-1} + d_2(\ln\alpha_H)_{\ell-2}]\,d\eta - \int_{i-1}^{i} f''(d_o f \\
&+ d_1 f_{\ell-1} + d_2 f_{\ell-2})d\eta
\end{aligned} \tag{4.10}$$

where the Taylor series described above can then be substituted into the integrals. The end result, after substantial algebra and manipulation, is the desired linear system of equations which can then be solved by standard matrix techniques. The complete sets of linearized equations can be found in Tong *et.al.* [1973] and the derivation of each one of these in Bartlett and Kendall [1967].

The technique used by BLIMPK to solve the system of equations is a simple Newton-Raphson technique, adapted to account for the fact that the matrix of coefficients is somewhat sparse in certain areas. This procedure is an iterative one which consists in solving for corrections to an approximate set of solutions and progressively letting the error approach some limit depending on the accuracy required. One should be

cautioned that the initial solution input to the program by the user should be as close as possible to the "expected" solution in order to avoid convergence problems. Unrealistic first guesses leading to over 100 iterations cause the code to "give up". However, once a solution is found within acceptable error bounds, the calculations proceed to the next downstream ξ station after the solution is dumped to an output file.

As far as the first step in the ξ direction is concerned, BLIMPK can perform a variety of initial calculations. In the case of a blunt body, an equilibrium stagnation point solution can be obtained depending on the nose radius and expanded to the appropriate boundary conditions at the boundary layer edge of the first station specified. For a sharp body, a similar solution is usually more appropriate, rather than specifying an arbitrarily small nose radius. The entropy might have to be adjusted between the tip and the first station should convergence problems arise because of conflicting edge conditions.

Chapter 5

BLIMPK Input Guide

The complete BLIMPK input guide is listed in Appendix A of Murray [1988] and will not be repeated in this report. Instead, the input files corresponding to the examples in the following section will be used to illustrate some of the more important parts of the BLIMPK input procedure. All of these input files are listed in Appendix B. It is hoped that by doing so, one can then easily adapt the input for the examples to new problems of interest. Most experiments performed in GALCIT's T5 hypervelocity shock tunnel will be similar in terms of chemistry models and flow conditions. Care should be taken, however, to follow the exact column format specified in the input guide as far as the thermodynamic data and reaction equations are concerned.

The first line in all input files is a comment line used as an identifier for the output. The main body of the input consists of several groups appended one after the other, since the original version of the code read in each one of these groups sequentially from separate files. All groups, except the ones containing the actual thermodynamic data, begin with "$GR" and end with "$END". Again, only a brief description of each group and a few comments will be given below.

$GR01 - *Control Cards*

The array KRI(i) contains 22 switches that control the way the rest of the input file is read in by the program. Of particular interest is KRI(5) which determines the treatment of the entropy layer. Setting KRI(5)=0 performs an isentropic expansion around the body with the entropy corresponding to the reference conditions input in $GR07. Setting KRI(5)=5 performs a nonisentropic expansion and the decrease in entropy between streamwise stations must be specified in $GR15 (DSIP(i)). Although the error is quite small, it is sometimes necessary to adjust the entropy from the stagnation point to the first streamwise station to account for the fact that BLIMPK always performs an equilibrium stagnation point solution not necessarily compatible with the edge conditions supplied by the user. In this case DSIP(1) should be to an appropriate value to get the correct edge conditions and the remaining DSIP(i) should be set to the "exact" entropy change required between stations, e.g. 0 for frozen conditions.

KRI(6) designates the body shape and can be set anywhere from 0 to 9. Axisymmetric and planar blunt bodies are 0 and 1 respectively, axisymmetric and planar sharp bodies are 2 and 3 respectively. The other options correspond to various bodies with transverse curvature effects and internal flows such as nozzles.

KRI(7) designates the type of flow to be considered. 0 and 1 correspond to laminar flow with reacting and non-reacting chemistry respectively. 2 and 3 correspond to turbulent flow with reacting and non-reacting chemistry respectively.

KRI(9) serves to specify the type of boundary conditions to be used. 2 should be used when the wall temperature T_w is specified. 7 is for an adiabatic wall.

KRI(11) should be set to 0 if the wall temperature is assigned and to 1 if the wall enthalpy is assigned.

KRI(12) is only relevant for reacting flows, i.e. KRI(7)=0 or 2. It should be set to 8 or 9 for nonequilibrium boundary layers with prescribed edge conditions, 9 being preferable when the nonisentropic expansion option is specified in KRI(5).

The remaining KRI(i) are mostly for debugging purposes and can be safely left as they are in the examples.

$GR02 - *Number of Elements and Stations*

NSP refers to the number of elements in the system not including electrons. In the case of nonequilibrium chemistry, NSP refers to number of species. For non-reacting flow it should be set to 1.

NS is the number of streamwise stations.

$GR03 - *Times and Stations*

S(i) is the streamwise distance in feet of each station. A blunt-body should start with S(1)=0 and a sharp body with S(1) set to a finite distance. The boundary layer is assumed to be similar up to and including this first station.

$GR04 - *Nodal Data*

NETA refers to the number of nodal points to be taken across the boundary layer including the wall and the edge. The maximum is 15 (see Chapter 4 for discussion on accuracy).

ETA(i) is the array with the coordinates in η space for the NETA points.

KAPPA and CBAR come from the α_H stretching as part of the coordinate transformation of the governing conservation equations (see equation 3.3). CBAR denotes the value of the velocity ratio u/u_e and KAPPA the number of the corresponding node.

$GR05 - *Body Shape Data*

For blunt bodies, the user must enter the effective nose radius RNOSE in feet and, in the case of a sphere-cone shape, the half-angle in degrees denoted by CONE.

ROKAP(i) is the spreading factor, i.e. the local body radius for axisymmetric bodies. In the case of a sharp cone, ROKAP(1) is set to minus the cone half-angle in degrees.

$GR07 - *Reference Conditions*

PTET(1) is the stagnation pressure in atmospheres. The surface pressure at each station entered later on in $GR15 will be input as a ratio of PTET

GE(1) is the corresponding stagnation enthalpy in BTU/lbm.

RADFL(1) is the incident radiation flux absorbed by the surface in BTU/sec-ft^2. As with pressure, the radiation flux at each station entered later on in $GR15 will be input as a ratio of RADFL

$GR08 - *Turbulent Flow Parameters*

Depending on the turbulence model desired (Kendall, Bushnell or Cebeci-Smith) these parameters can be changed. All examples included in the following sections use the Cebeci-Smith model. The only parameter to change is RETR which refers to the Reynolds number based on momentum thickness where the calculation should switch from laminar to turbulent. A negative integer can also be input to indicate the station number where to make the switch.

$GR09 - *First Guesses*

Depending on the chemistry option guesses for either only the wall enthalpy GW or both the wall enthalpy GW and wall species concentrations SPFG(i) must be entered.

$GR10 - *Property Data for Non-reacting Boundary Layer*

In the first part of this group, the user must enter fits for the Prandtl number and the viscosity. The coefficients for the Prandtl number expression

$$\mathrm{PR} = \mathrm{PRDNUM} + \mathrm{PRA} * T^{\mathrm{PRB}} + \mathrm{PRC} * T^{\mathrm{PRD}}$$

with the temperature T in deg-R, are input in the following order: PRDNUM, PRA, PRB, PRC and PRD. If the Prandtl number is constant, only PRDNUM needs to be specified.

The coefficients for the viscosity expression

$$\mu = \frac{\mathrm{VMUA} * T^{\mathrm{VMUB}}}{\mathrm{VMUC} * T + \mathrm{VMUD}}$$

with the temperature T in deg-R and the viscosity μ in lbm/s-ft, are input in the following order: VMUA, VMUB, VMUC and VMUD.

Finally, NC, the number of components in the gas mixture, must be specified before the $END.

In the second part of this group, the actual thermodynamic data is entered. This consists of curve fits as well. However, the user can enter different fits over different temperature ranges. The input is separated by component of the gas mixture. Each entry is comprised of the component name, molecular weight, mass (or mole) fraction and the fit coefficients EF(1) through EF(6) for the different temperature ranges. Care must be taken in this part to follow the correct columnar alignment. This part of the group does not begin with

a $GR nor does it end with a $END. Notice also that all thermodynamic data is input in S.I. units since most of it comes from standard JANAF tables.

$GR11 - *Elemental Data for Reacting Boundary Layer*

In this group, for most cases, only the number of species must be entered along with the name and mass (or mole) fraction of each one present in the boundary layer edge. Care must also be taken in this group to follow the correct columnar alignment. This group does not begin with a $GR nor does it end with a $END either.

$GR13 - *Thermochemical Data for Reacting Boundary Layer*

The input for this section is similar to that in $GR10 except that fits are not needed for the Prandtl number and viscosity since they are calculated with built-in mixture formulas depending on the local gas composition which changes within the boundary layer. Care must also be taken in this group to follow the correct columnar alignment. This group does not begin with a $GR nor does it end with a $END.

$GR14 - *Kinetic Data for Reacting Boundary Layer*

The first line of this group consists of three integers. The first designates the number of surface reactions to be read below, the second the number of gas phase reactions and the third whether to consider variable rates. The typical format is best understood by looking at the examples in Appendix B.2 or B.4 and by referring to the actual input guide since the columnar alignment is also critical here. This group does not begin with a $GR nor does it end with a $END.

$GR15 - *Streamwise Distribution of Edge Conditions*

For non-reacting flows, only the static pressure PRE(1) at the boundary layer edge for each streamwise station is entered. It should be given in nondimensional form, normalized by the reference pressure PTET in atmospheres given in $GR07 above. One can also specify the entropy decrease between stations, DSIP(1), depending on the value of KRI(5) entered in $GR01.

The only additions for reacting flow are that the edge species concentrations at each station must be input as well.

$GR16 - *Streamwise Distribution of Wall Conditions*

Depending on the type of wall boundary conditions, one can enter either the enthalpy HW in BTU/lbm or the temperature TW in deg-R.

BLIMPK Output File

A few words on the output, although large self-explanatory and easy to follow, might also be appropriate. At each streamwise position, a complete set of boundary layer parameters is output once satisfactory

convergence is achieved within an acceptable error bound. Parameters include, among others, velocity, temperature, density, Chapman-Rubesin parameter and depending on the problem, all species concentrations and corresponding derivatives at each η node. Boundary layer displacement and momentum thicknesses are also output at each station.

Of particular interest to many problems is the wall heat transfer. BLIMPK outputs the total but also lists the individual contributions to isolate the different effects. The actual heat flux to the wall is given by

$$q_w = q_e - \dot{m}h - \epsilon\sigma T^4 + \dot{m}h_o + q_r$$

where,

$$q_e = k\frac{\partial T}{\partial y} + \rho D_{12}\sum h_i \frac{\partial K_i}{\partial y}$$

and q_r is the incident radiation. The emitted radiation is given by $\epsilon\sigma T^4$ and the heat carried away by blowing by $\dot{m}(h - h_o)$.

Chapter 6

Examples

6.1 Air Boundary Layer on a Sharp Cone

The following examples are simulations of shots 671 and 675 performed in the T5 hypervelocity shock tunnel. In both cases, the freestream Mach number was around M=5. Shot 671 is a high pressure (P_o=78.6 MPa) - high enthalpy shot (h_o=21.3 MJ/kg). The corresponding Reynolds number based on the boundary layer edge properties is Re/L=3.5$\times 10^6$ m^{-1} and the flow is laminar over the entire model surface. Shot 675 is a medium pressure (P_o=58.5 MPa) - low enthalpy shot (h_o=10.5 MJ/kg). The corresponding Reynolds number is Re/L=5.5$\times 10^6$ m^{-1} and although the flow starts out laminar, it transitions to turbulence around Re_{tr}=2.9$\times 10^6$. These observations about the state of the boundary layer are all obtained from experimental surface heat transfer measurements. BLIMPK can then be used to compute the corresponding boundary layer profiles at each measurement station.

All numbers needed to write the proper input for BLIMPK are calculated directly or indirectly from basic T5 tunnel parameters such as the shock speed v_s and stagnation pressure P_o. The complete set of boundary layer edge properties are obtained assuming the composition is identical to the freestream and solving the Taylor-Maccoll equations for a 5° half-angle cone at Mach 5. These conditions are summarized for the two shots considered in the table below.

Shot	P_o (MPa)	h_o (MJ/kg)	P_e (kPa)	T_e (K)	M_e	Re/L ($\times 10^6 m^{-1}$)
671	78.6	21.3	62.0	3440	4.84	3.5
675	58.5	10.5	39.7	1740	5.00	5.5

Table 6.1 - Flow Conditions for shots 671 and 675

6.1.1 Frozen Chemistry

The BLIMPK input file for shot 671 with frozen chemistry is listed in Appendix B.1. The file for shot 675 is not listed since it is almost exactly the same except that the calculation is forced to include turbulence at a station close to where the experiment showed transition to have taken place.

Velocity, temperature and density profiles are shown in Figures 6.1(a)-(c) and 6.2(a)-(c) for shot 671 and 675 respectively. They correspond to three different streamwise locations on the cone. These are typical profiles for shock tunnel generated boundary layers, i.e. the temperature increases rapidly from the very cold wall to a maximum close to the wall before decreasing to the hot freestream. It should be noted, however that the maximum temperature is not that much higher than the freestream. The profiles for 671 are obviously all laminar but the temperature plots for shot 675 illustrate well the thickening of the boundary layer once it becomes turbulent.

Species concentration profiles are not shown since the mass fractions are assumed to be frozen throughout the layer. It is quite obvious that this is not very realistic because the high temperatures, especially in tha case of shot 671, are likely to cause further dissociation, of diatomic oxygen for example, inside the boundary layer. For this reason and because surface catalysis might promote the opposite, i.e. recombination, nonequilibrium calculations are necessary as well.

6.1.2 Nonequilibrium Chemistry

The BLIMPK input file for shot 671 with nonequilibrium chemistry is listed in Appendix B.2. The listing accounts for a fully catalytic wall. A noncatalytic wall can be simulated by changing the reaction rate from 1×10^{6} to 1×10^{-6}. Again, the file for shot 675 is not listed since it is almost exactly the same except that the calculation is forced to include turbulence.

The velocity, temperature and density profiles are practically unchanged from those obtained assuming frozen flow and are therefore not plotted here below. The only difference is a slight increase in the maximum temperature for the noncatalytic case and a slightly larger increase for the fully catalytic case. The species concentration profiles, however, reveal more and are plotted for shot 671 in Figures 6.3(a)-(b) for the fully catalytic wall and the noncatalytic wall respectively. Figures 6.4(a)-(c) combine both types of wall for shot 675 on the same set of plots. On all plots, the vertical profile represents the frozen edge concentration.

One should first note that the freestream is highly dissociated in the high enthalpy case since there is substantially more atomic oxygen O at the boundary layer edge for shot 671. When the wall is catalytic, as expected, all of it recombines to give molecular oxygen O_2. A bit of NO is formed because of the plentiful supply of O and some dissociation of N_2 (not shown) at the higher temperatures but quickly decreases close to the wall as the N recombines as much as the O. The gas is entirely made up of diatomic oxygen and nitrogen at the wall.

In the noncatalytic case for shot 671, there is no possibility of recombination at the wall so that O_2 dissociates from the edge down as the temperature goes up. However, once it approaches the cold wall, the little O that was formed recombines. There is also a slight increase in NO. In the case of shot 675, the temperatures reached inside the boundary layer are nowhere near the levels needed for these same dissociation/recombination reactions to be efficient and the effects, as can be seen in the plots, are not as severe. Heat transfer rates computed by BLIMPK, as compared with the experiments, are shown in Figures 6.5 and 6.6 for shots 671 and 675 respectively.

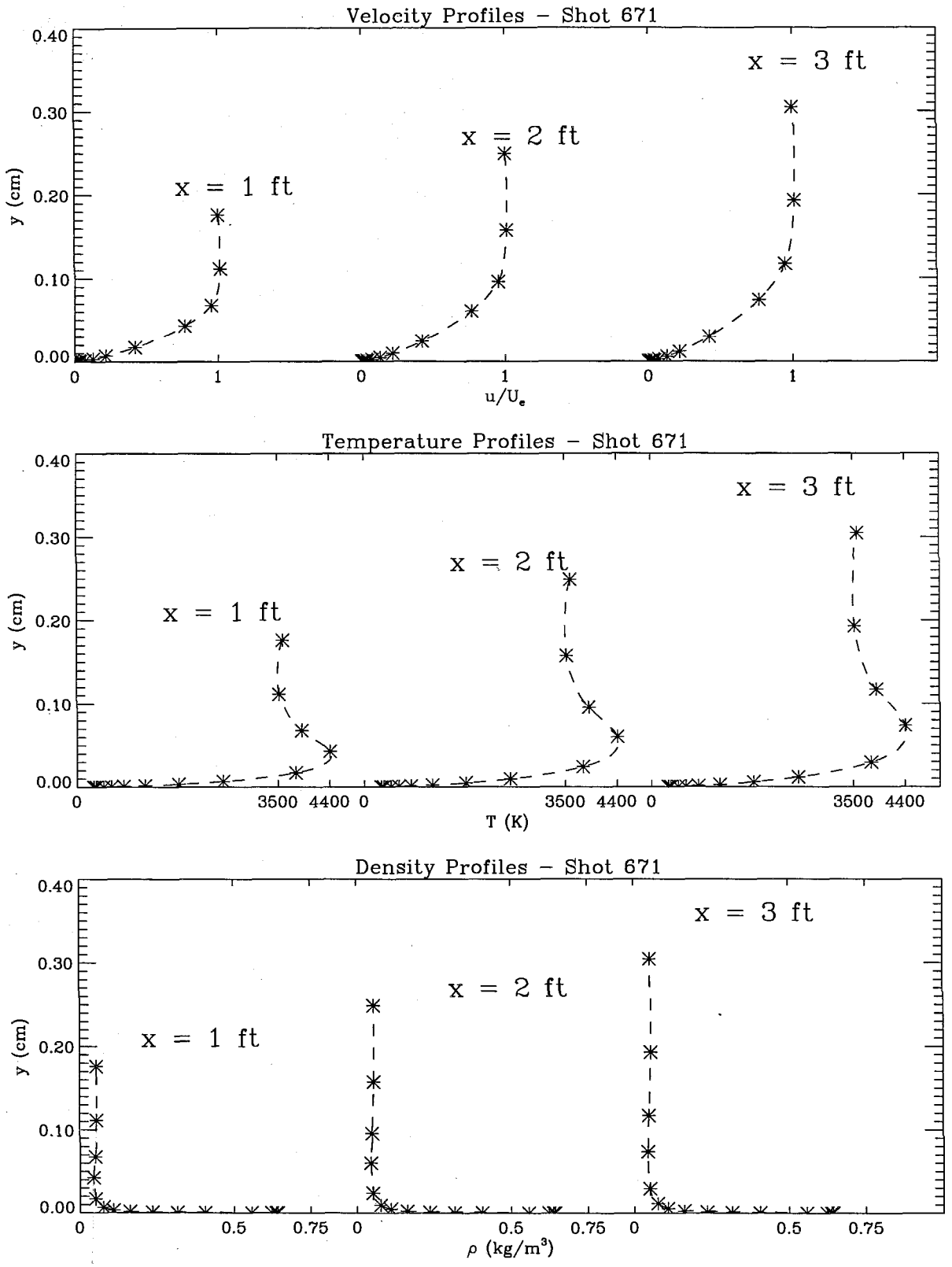

Figures 6.1(a)-(c) - Velocity, temperature and density profiles for shot 671

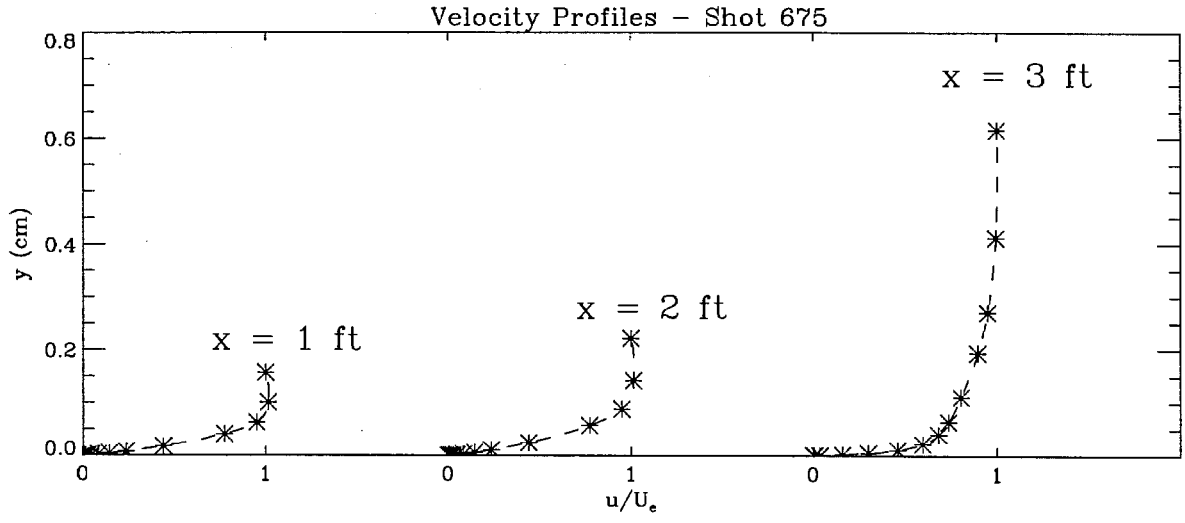

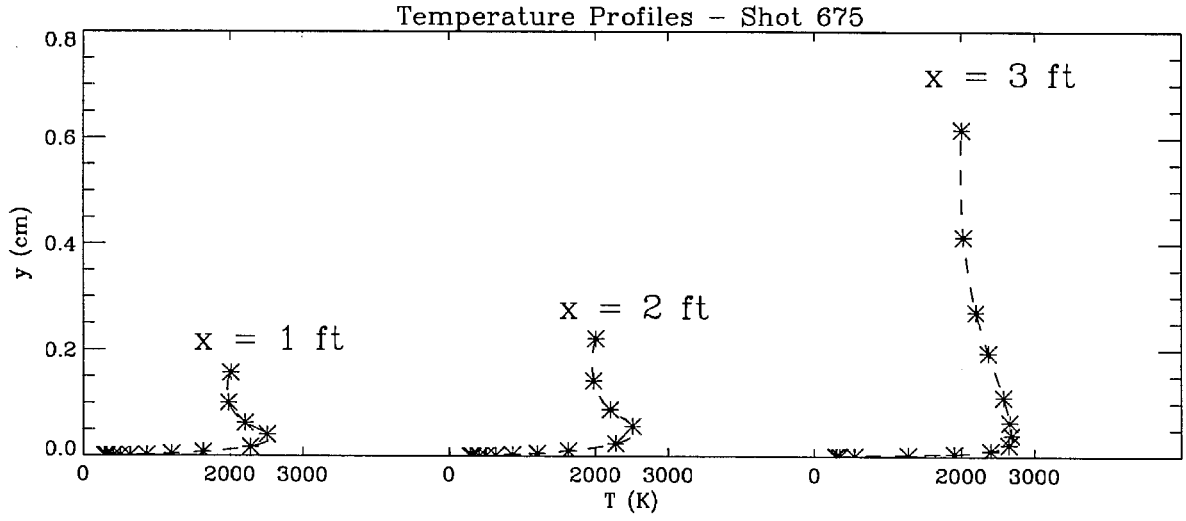

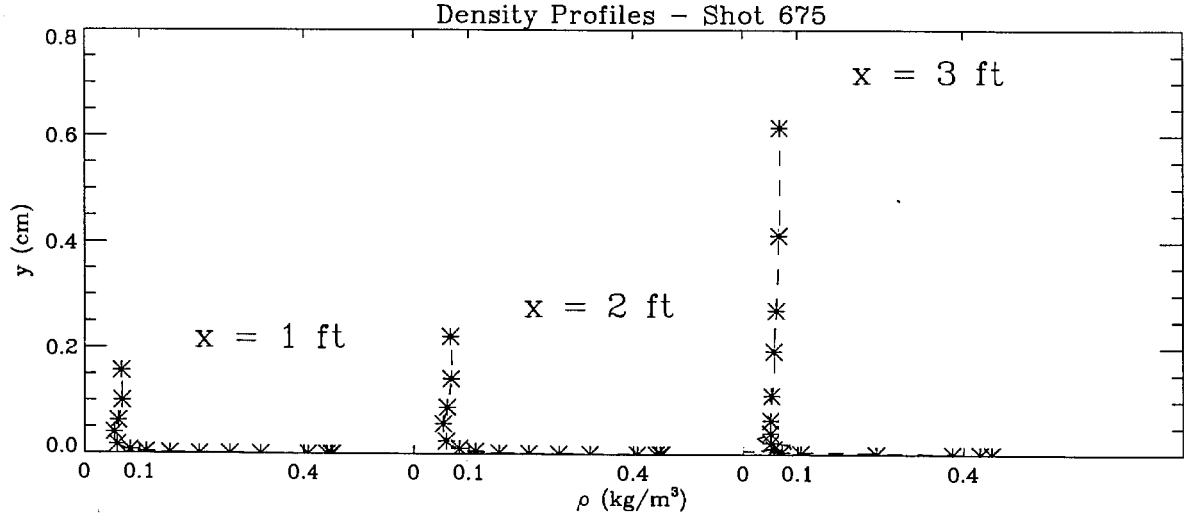

Figures 6.2(a)-(c) - Velocity, temperature and density profiles for shot 675

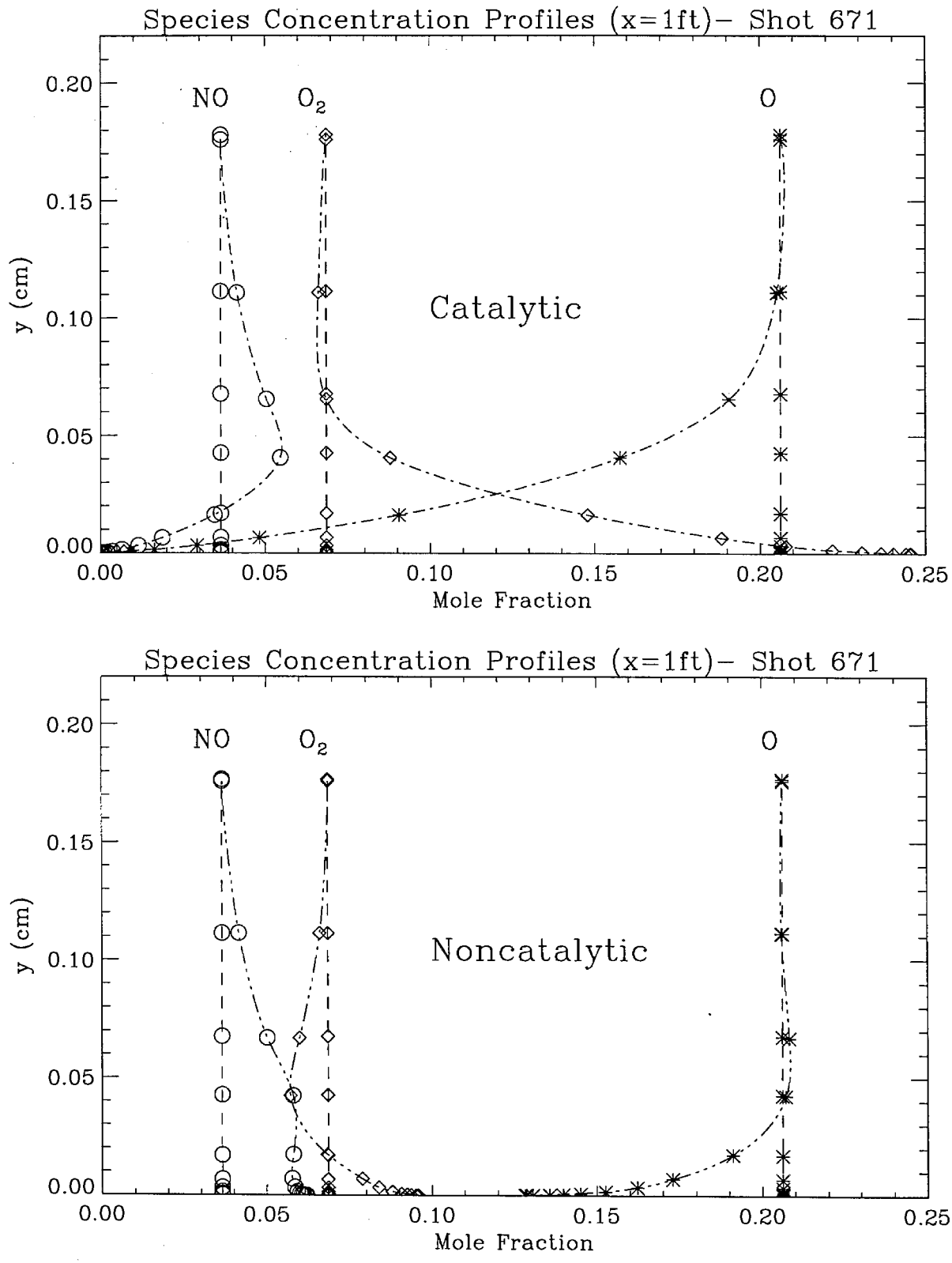

Figures 6.3(a)-(b) - Catalytic and noncatalytic species concentrations for shot 671

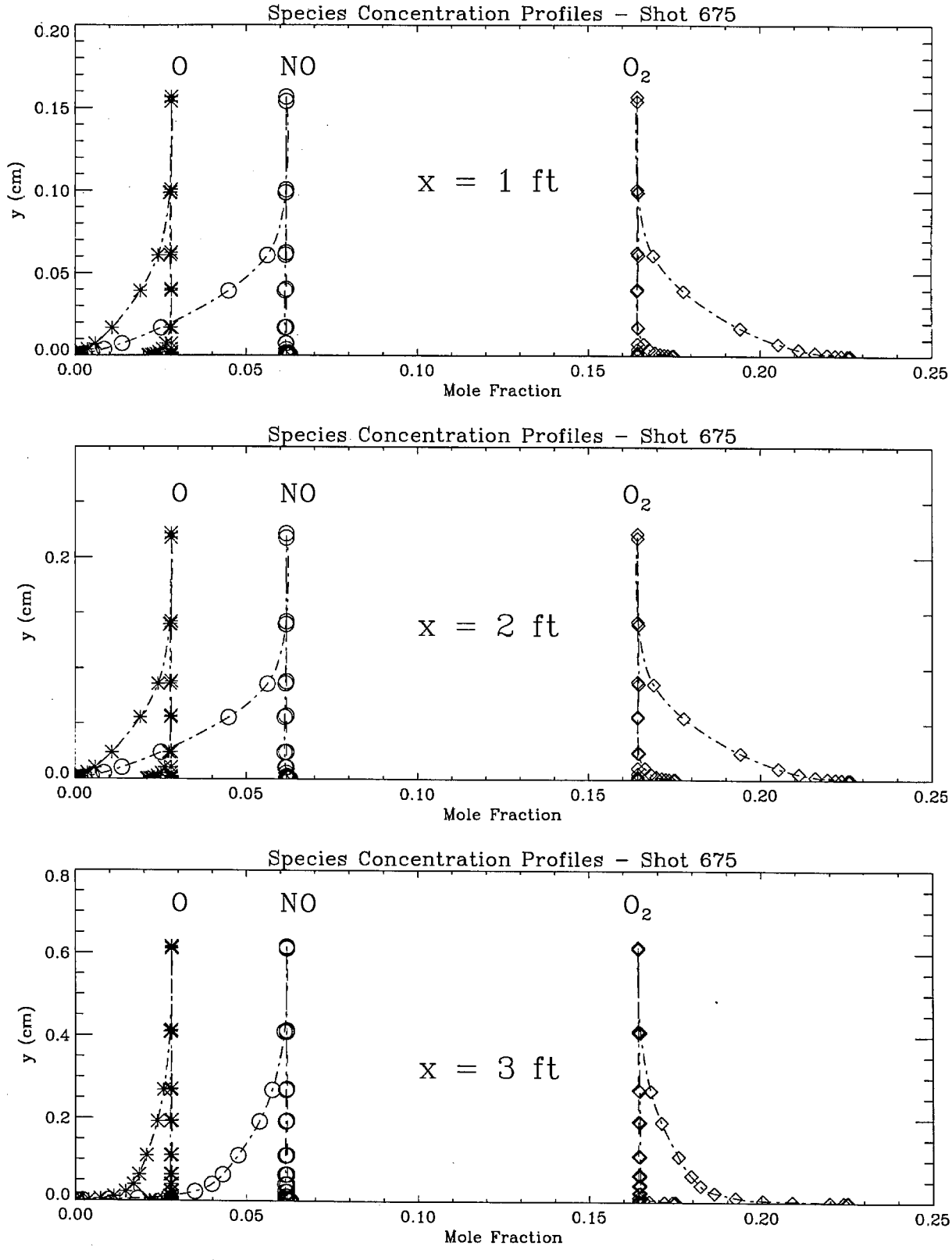

Figures 6.4(a)-(c) - Catalytic and noncatalytic species concentrations for shot 675
(Noncatalytic results are barely distinguishable from the frozen line except close to the wall)

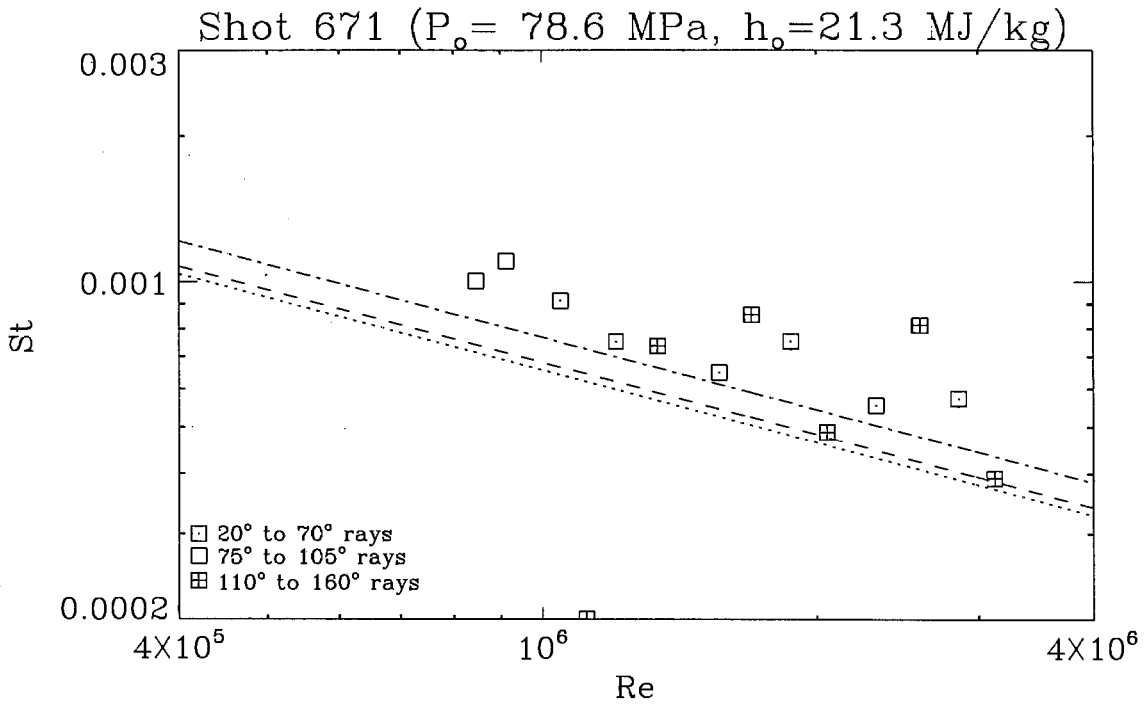

Figure 6.5 - Experimental heat transfer distribution for shot 671
Lines represent BLIMPK computations: frozen, noncatalytic and catalytic (bottom to top)

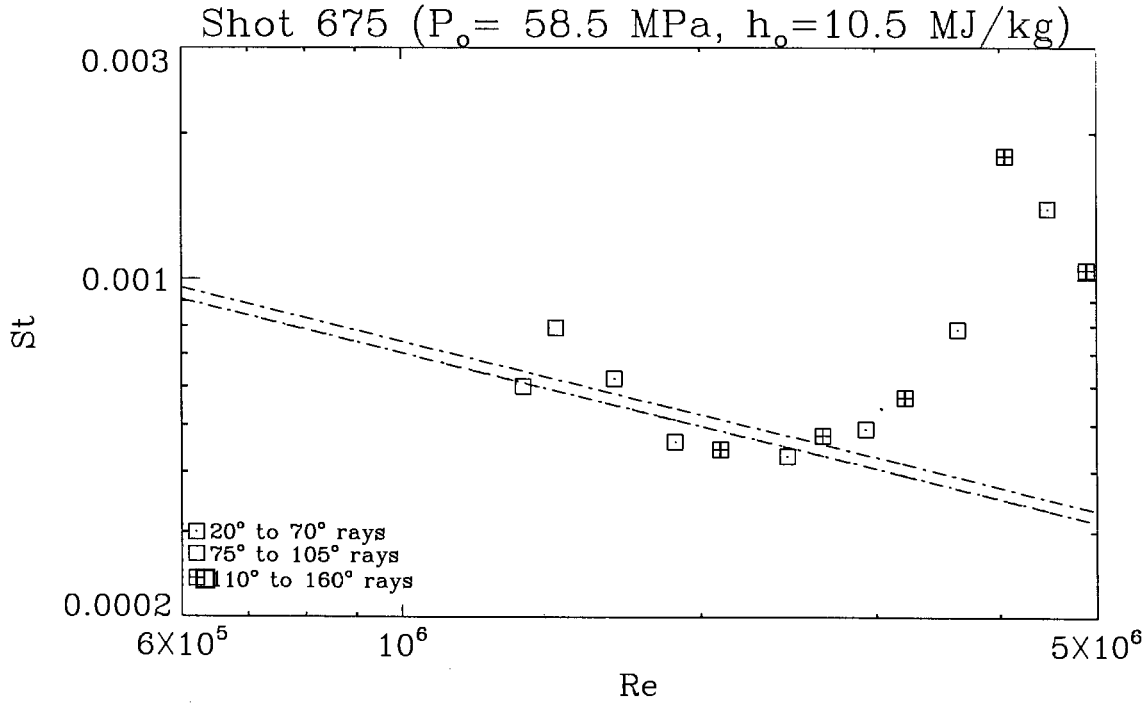

Figure 6.6 - Experimental heat transfer distribution for shot 675
Lines represent BLIMPK computations: frozen, noncatalytic and catalytic (bottom to top)

6.2 Carbon Dioxide Boundary Layer on a Sharp Cone

The following examples are simulations of shot 1144. Shot 1144 is a high pressure (P_o=79.2 MPa) - high enthalpy shot (h_o=9.1 MJ/kg). The corresponding Reynolds number based on the boundary layer edge properties is Re/L=8.3×10^6 m^{-1} and the flow is laminar over the entire model surface. It should be pointed out that high enthalpy in the case of carbon dioxide is quite different than for air. This is because a similar degree of dissociation can be achieved for a much lower shock speed, hence the lower value of h_o.

Shot	P_o (MPa)	h_o (MJ/kg)	P_e (kPa)	T_e (K)	M_e	Re/L ($\times 10^6 m^{-1}$)
1144	79.2	9.1	83.9	2390	4.38	8.3

Table 6.2 - Flow Conditions for shot 1144

6.2.1 Frozen Chemistry

The BLIMPK input file for shot 1144 with frozen chemistry is listed in Appendix B.3.

Velocity, temperature and density profiles are shown in Figures 6.7(a)-(c). They correspond to the same three streamwise locations on the cone as in the air examples. The flow is laminar everywhere and there is no qualitative difference compared to the air shots except that the maximum temperature appears to be far less pronounced.

6.2.2 Nonequilibrium Chemistry

The BLIMPK input file for shot 1144 with nonequilibrium chemistry is listed in Appendix B.4. The listing also accounts for a fully catalytic wall. A noncatalytic wall can be simulated by changing the reaction rate from 1×10^6 to 1×10^{-6}.

As with air, the velocity, temperature and density profiles are practically unchanged from those obtained assuming frozen flow and are therefore not plotted here below. The species concentration profiles reveal little and are plotted in Figure 6.8 for one station only. The results for the fully catalytic wall and the noncatalytic wall are indistinguishable. The vertical profile again represents the frozen edge concentration. The mole fraction of CO_2 is not shown.

The heat transfer rate computed by BLIMPK is shown in Figures 6.9 for this shot and falls far below the experimental results. This is because the chemistry is probably inadequately modeled, in particular, at the level of the surface reactions. The actual gas phase reaction rates could probably also be improved by covering specifically the temperature range of this problem. However, little is known of the chemistry of high enthalpy carbon dioxide flows and more work in the future can only add to the understanding of this type of boundary layer.

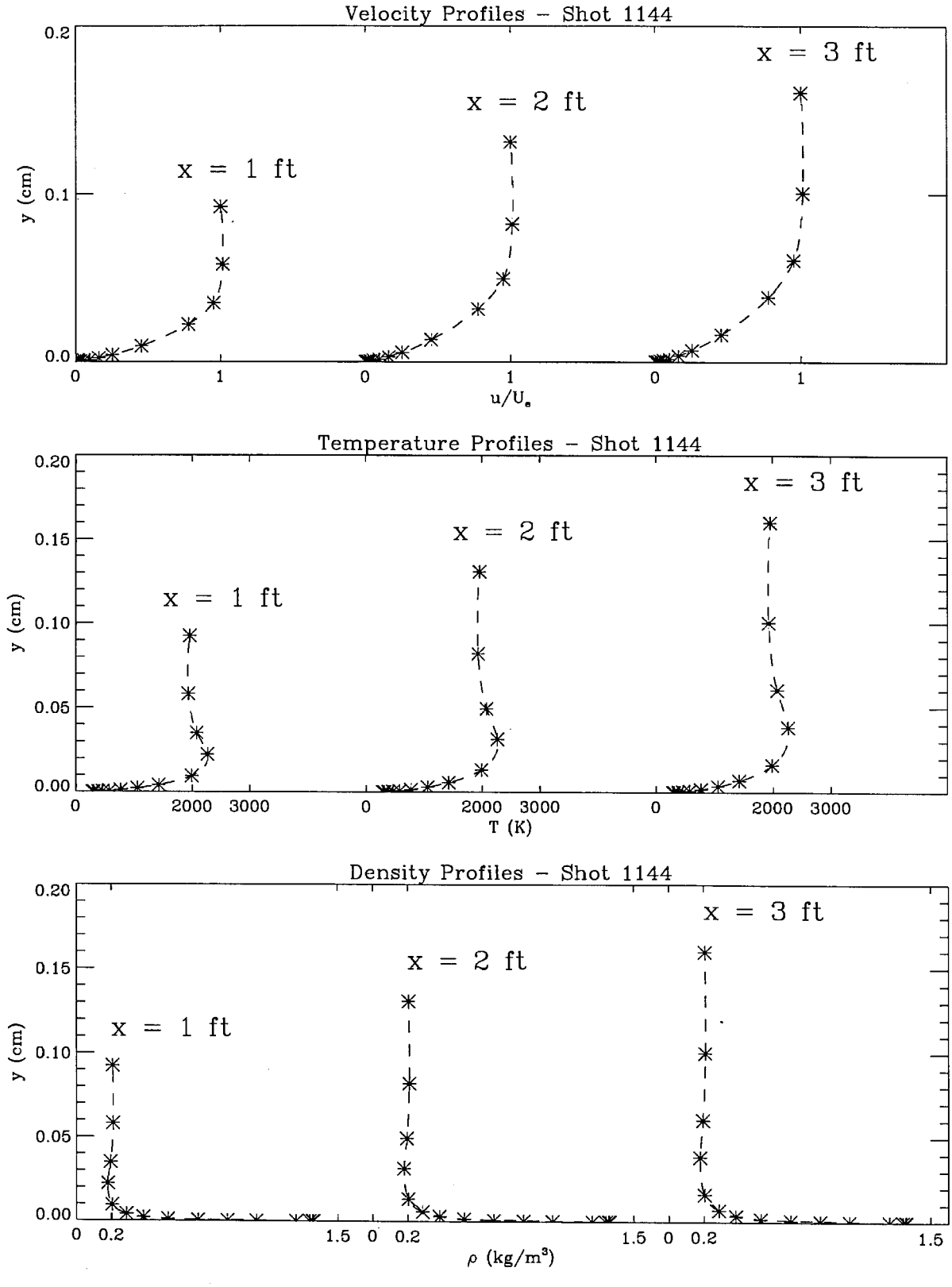

Figures 6.7(a)-(c) - Velocity, temperature and density profiles for shot 1144

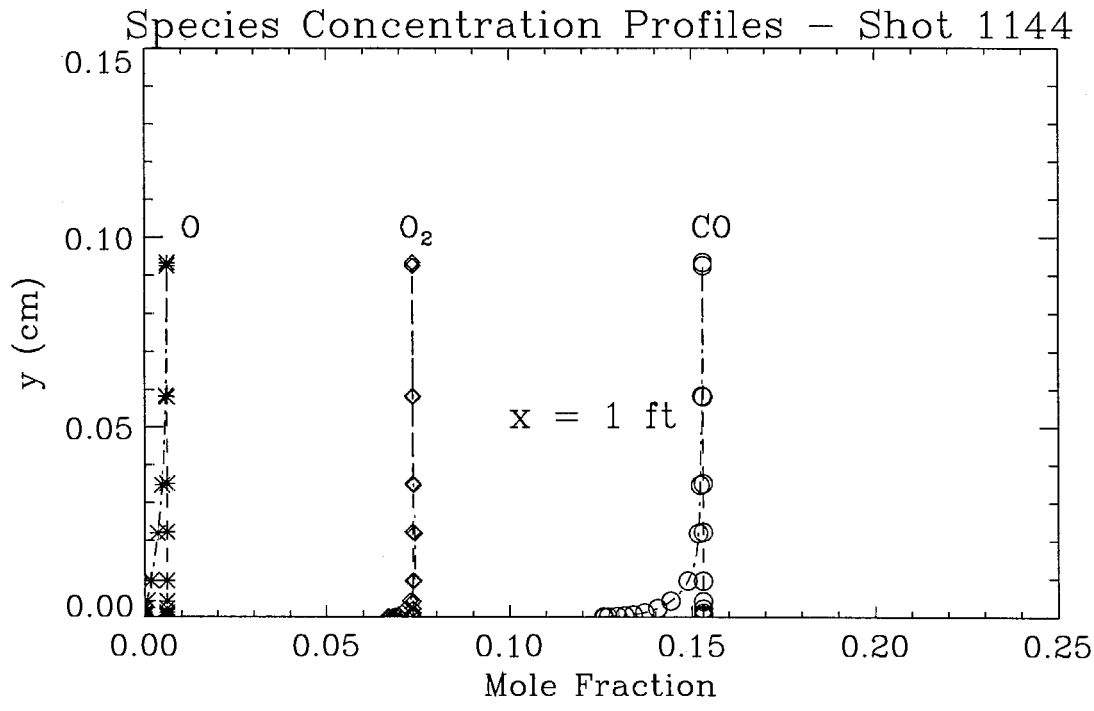

Figures 6.8 - Catalytic and noncatalytic species concentrations for shot 1144
(Noncatalytic results are not distinguishable from the catalytic ones)

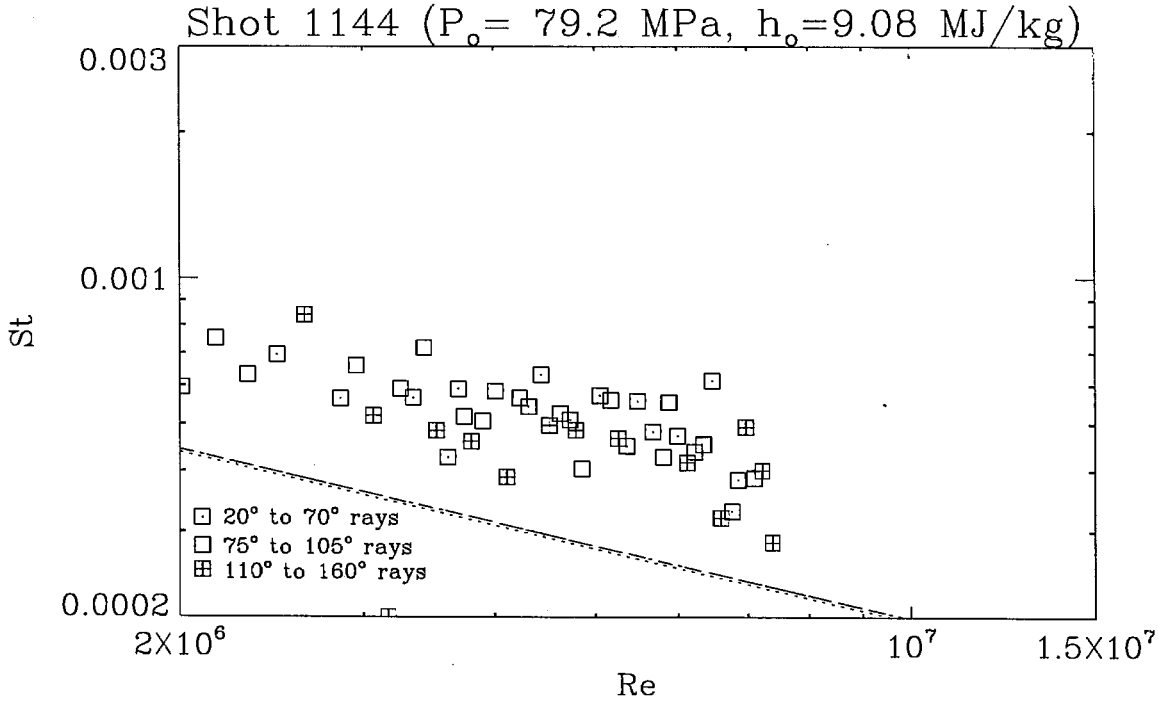

Figure 6.9 - Experimental heat transfer distribution for shot 1144
Lines represent BLIMPK computations: frozen, noncatalytic and catalytic (bottom to top)

Chapter 7

Conclusions

A brief review of the BLIMPK - Boundary Layer Integral Matrix Procedure with Kinetics - program has been given and examples of actual experiments run in the T5 hypervelocity shock tunnel have been simulated.

The conservation equations - mass, momentum, energy and species - relevant to hypervelocity flows were first listed and discussed. The equations represent laminar or turbulent flows and take into account gas phase as well as surface reactions. To simplify the solution procedure the equations are first transformed from the standard (s,y) physical space to a (ξ, η) computational space with a modified Levy-Lees transformation. The discretization in the transverse direction is done by splitting the boundary layer into strips and spline fitting primary variables in between these strips with Taylor series. Discretization in the streamwise direction is achieved using standard finite difference techniques. After applying a square weighting function over the entire boundary layer and integrating across a single strip, the equations are effectively linearized and the entire problem becomes one of inverting a very large but sparse matrix. A Newton-Raphson iteration procedure is then used for each streamwise station until the error is brought down to a tolerable level and a solution is then output.

Examples of T5 flows simulated with BLIMPK include air and carbon dioxide hypervelocity flows over a sharp 5° half-angle cone. Computations are shown including frozen and nonequilibrium chemistry. In the case of nonequilibrium chemistry, both catalytic and noncatalytic walls are considered. High enthalpy air flows are quite complex as the results indicate. The high temperatures inside the boundary layer and the wall reactions severely affect the species concentrations and the heat transfer level although velocity, temperature and density profiles seem almost unchanged. Air results with a catalytic wall come closest to the experimental numbers. Carbon dioxide flows appear, however, to be much harder to simulate most probably because of poor chemistry modeling of the gas phase and, especially, surface reactions.

References

Anderson, J. D. 1989 Hypersonic and High Temperature Gas Dynamics, McGraw-Hill, New York

Bartlett, E. P. and Kendall, R. M. 1967 "An Analysis of the Coupled Chemically Reacting Boundary Layer and Charring Ablator, Part III," Nonsimilar Solution of the Multicomponent Laminar Boundary Layer by an Integral Matrix Method, Aerotherm Final Report 66-7, Part III, Aerotherm Corporation, March 1967 (also NASA CR-1062)

Chen, Y.-K., Henline, W. D., Stewart, D. A. and Candler, G. V. 1993 "Navier-Stokes Solutions with Surface Catalysis for Martian Atmospheric Entry," AIAA J. Spacecraft and Rockets, vol. 30, no. 1, January-February 1993

Dorrance, W. H. 1962 Viscous Hypersonic Flow, McGraw-Hill, New York

Evans, R. M. 1975 "JANAF Boundary Layer Integral Matrix Procedure," Aerotherm Final Report 75-152, Acurex Corporation, July 1975 (also NASA CR-143947)

Lees, L. 1956 "Laminar Heat Transfer Over Blunt-Nosed Bodies at Hypersonic Flight Speeds," Jet Propulsion, vol. 26, no. 4, April 1956

Murray, A. L. 1988 "Further Enhancements of the BLIMP Computer Code and User's Guide," Aerotherm Final Report 88-12/ATD, Acurex Corporation, June 1988 (also AFWAL TR-88-3010)

Park, C., Howe, J. T., Jaffe, R. L. and Candler, G. V. 1994 "Review of Chemical-Kinetic Problems of Future NASA Missions, II: Mars Entries," AIAA J. Thermophysics and Heat Transfer, vol. 8, no. 1, January-March 1994

Tong, H., Buckingham, A. C. and Morse H. L. 1973 "Nonequilibrium Chemistry Boundary Layer Integral Matrix Procedure," Aerotherm Final Report 73-67, Acurex Corporation, July 1973 (also NASA CR-134039)

Appendix A

Gas Phase and Surface Reactions

The rate constants in these tables have been taken from the following reports:

- Tong *et.al.* [1973]
- Chen *et.al.* [1993]
- Park *et.al.* [1994]

A.1 Air - Reaction Rates

Gas Phase Reactions, k_f ($cm^3 mole^{-1} s^{-1}$ or $cm^6 mole^{-2} s^{-1}$)

REACTION	BLIMP Kinetics	Park Kinetics	McKenzie Kinetics
$O_2 + N \rightarrow 2\,O + N$	$3.61e18\ T^{-1.0} e^{-59,400/T}$	$1.0e22\ T^{-1.5} e^{-59,750/T}$	$9.05e18\ T^{-1.0} e^{-59,370/T}$
$O_2 + O \rightarrow 2\,O + O$	$90.25e18\ T^{-1.0} e^{-59,400/T}$	$1.0e22\ T^{-1.5} e^{-59,750/T}$	$9.05e18\ T^{-1.0} e^{-59,370/T}$
$O_2 + NO \rightarrow 2\,O + NO$	$3.61e18\ T^{-1.0} e^{-59,400/T}$	$2.0e21\ T^{-1.5} e^{-59,750/T}$	$9.05c18\ T^{-1.0} e^{-59,370/T}$
$O_2 + O_2 \rightarrow 2\,O + O_2$	$32.5e18\ T^{-1.0} e^{-59,400/T}$	$2.0e21\ T^{-1.5} e^{-59,750/T}$	$9.05e18\ T^{-1.0} e^{-59,370/T}$
$O_2 + N_2 \rightarrow 2\,O + N_2$	$7.22e18\ T^{-1.0} e^{-59,400/T}$	$2.0e21\ T^{-1.5} e^{-59,750/T}$	$9.05e18\ T^{-1.0} e^{-59,370/T}$
$N_2 + O \rightarrow 2\,N + O$	$1.92e17\ T^{-0.5} e^{-113,100/T}$	$3.0e22\ T^{-1.6} e^{-113,200/T}$	$2.46e19\ T^{-1.0} e^{-113,200/T}$
$N_2 + NO \rightarrow 2\,N + NO$	$1.92e17\ T^{-0.5} e^{-113,100/T}$	$7.0e21\ T^{-1.6} e^{-113,200/T}$	$2.46e19\ T^{-1.0} e^{-113,200/T}$
$N_2 + O_2 \rightarrow 2\,N + O_2$	$1.92e17\ T^{-0.5} e^{-113,100/T}$	$7.0e21\ T^{-1.6} e^{-113,200/T}$	$2.46e19\ T^{-1.0} e^{-113,200/T}$
$N_2 + N_2 \rightarrow 2\,N + N_2$	$4.80c17\ T^{-0.5} e^{-113,100/T}$	$7.0e21\ T^{-1.6} e^{-113,200/T}$	$2.46e19\ T^{-1.0} e^{-113,200/T}$
$N_2 + N \rightarrow 3\,N$	$4.15c22\ T^{-1.5} e^{-113,100/T}$	$3.0e22\ T^{-1.6} e^{-113,200/T}$	$2.46e19\ T^{-1.0} e^{-113,200/T}$
$NO + N \rightarrow N + O + N$	$79.4e20\ T^{-1.5} e^{-76,500/T}$	$1.1e17\ T^{0.0} e^{-75,500/T}$	$4.09e18\ T^{-1.0} e^{-75,330/T}$
$NO + O \rightarrow N + O + O$	$79.4e20\ T^{-1.5} e^{-76,500/T}$	$1.1e17\ T^{0.0} e^{-75,500/T}$	$4.09e18\ T^{-1.0} e^{-75,330/T}$
$NO + NO \rightarrow N + O + NO$	$79.4e20\ T^{-1.5} e^{-76,500/T}$	$1.1e17\ T^{0.0} e^{-75,500/T}$	$4.09e18\ T^{-1.0} e^{-75,330/T}$
$NO + O_2 \rightarrow N + O + O_2$	$3.97e20\ T^{-1.5} e^{-76,500/T}$	$5.0e15\ T^{0.0} e^{-75,500/T}$	$4.09e18\ T^{-1.0} e^{-75,330/T}$
$NO + N_2 \rightarrow N + O + N_2$	$3.97e20\ T^{-1.5} e^{-76,500/T}$	$5.0e15\ T^{0.0} e^{-75,500/T}$	$4.09e18\ T^{-1.0} e^{-75,330/T}$
$NO + O \rightarrow O_2 + N$	$3.18e9\ T^{1.0} e^{-19,700/T}$	$8.4e12\ T^{0.0} e^{-19,450/T}$	$2.98e11\ T^{0.5} e^{-19,460/T}$
$N_2 + O \rightarrow NO + N$	$6.75e13\ T^{0.0} e^{-37,500/T}$	$6.4e17\ T^{-1.0} e^{-38,370/T}$	$7.35e11\ T^{0.5} e^{-37,940/T}$

Surface Reactions

REACTION	Fully Catalytic Wall	Noncatalytic Wall
$O \rightarrow \frac{1}{2} O_2$	1e6	1e-6
$N \rightarrow \frac{1}{2} N_2$	1e6	1e-6
$NO \rightarrow \frac{1}{2} O_2 + \frac{1}{2} N_2$	1e6	1e-6

A.2 CO_2 - Reaction Rates

Gas Phase Reactions, k_f ($cm^3mole^{-1}s^{-1}$ or $cm^6mole^{-2}s^{-1}$)

REACTION	BLIMP Kinetics	Park Kinetics	McKenzie Kinetics
$O_2 + O \rightarrow 2\,O + O$	90.25e18 $T^{-1}e^{-59,400/T}$	1.0e22 $T^{-1.5}e^{-59,750/T}$	9.05e18 $T^{-1.0}e^{-59,370/T}$
$O_2 + C \rightarrow 2\,O + C$	N/A	1.0e22 $T^{-1.5}e^{-59,750/T}$	9.05e18 $T^{-1.0}e^{-59,370/T}$
$O_2 + O_2 \rightarrow 2\,O + O_2$	32.5e18 $T^{-1}e^{-59,400/T}$	2.0e21 $T^{-1.5}e^{-59,750/T}$	9.05e18 $T^{-1.0}e^{-59,370/T}$
$O_2 + CO \rightarrow 2\,O + CO$	N/A	2.0e21 $T^{-1.5}e^{-59,750/T}$	9.05e18 $T^{-1.0}e^{-59,370/T}$
$O_2 + CO_2 \rightarrow 2\,O + CO_2$	N/A	2.0e21 $T^{-1.5}e^{-59,750/T}$	9.05e18 $T^{-1.0}e^{-59,370/T}$
$CO_2 + O \rightarrow CO + O + O$	N/A	3.70e14 $T^{0.0}e^{-52,500/T}$	1.20e11 $T^{0.5}e^{-34,340/T}$
$CO_2 + C \rightarrow CO + O + C$	N/A	3.70e14 $T^{0.0}e^{-52,500/T}$	1.20e11 $T^{0.5}e^{-34,340/T}$
$CO_2 + O_2 \rightarrow CO + O + O_2$	N/A	3.70e14 $T^{0.0}e^{-52,500/T}$	1.20e11 $T^{0.5}e^{-34,340/T}$
$CO_2 + CO \rightarrow CO + O + CO$	N/A	3.70e14 $T^{0.0}e^{-52,500/T}$	1.20e11 $T^{0.5}e^{-34,340/T}$
$CO_2 + CO_2 \rightarrow CO + O + CO_2$	N/A	3.70e14 $T^{0.0}e^{-52,500/T}$	1.20e11 $T^{0.5}e^{-34,340/T}$
$CO + O \rightarrow C + O + O$	N/A	3.40e20 $T^{-1.0}e^{-129,000/T}$	4.48e19 $T^{-1.0}e^{-128,900/T}$
$CO + C \rightarrow C + O + C$	N/A	3.40e20 $T^{-1.0}e^{-129,000/T}$	4.48e19 $T^{-1.0}e^{-128,900/T}$
$CO + O_2 \rightarrow C + O + O_2$	N/A	2.30e19 $T^{-1.0}e^{-129,000/T}$	4.48e19 $T^{-1.0}e^{-128,900/T}$
$CO + CO \rightarrow C + O + CO$	N/A	4.48e19 $T^{-1.0}e^{-129,000/T}$	4.48e19 $T^{-1.0}e^{-128,900/T}$
$CO + CO_2 \rightarrow C + O + CO_2$	N/A	2.30e19 $T^{-1.0}e^{-129,000/T}$	4.48e19 $T^{-1.0}e^{-128,900/T}$
$CO_2 + O \rightarrow CO + O_2$	N/A	1.70e13 $T^{0.0}e^{-26,500/T}$	2.54e11 $T^{0.5}e^{-27,690/T}$
$CO + O \rightarrow C + O_2$	N/A	3.90e13 $T^{-0.18}e^{-69,200/T}$	2.73e12 $T^{0.5}e^{-69,540/T}$
$CO + CO \rightarrow CO_2 + C$	N/A	2.33e9 $T^{0.5}e^{-65,710/T}$	2.33e9 $T^{0.5}e^{-65,710/T}$

Surface Reactions

REACTION	Fully Catalytic Wall	Noncatalytic Wall
$C + O \rightarrow CO$	1e6	1e-6
$CO + O \rightarrow CO_2$	1e6	1e-6
$O \rightarrow \frac{1}{2}\,O_2$	1e6	1e-6

Appendix B

BLIMPK Input Files for Sharp Cone

Note: Although the rows of the following input files are in the correct order, care must be taken to follow the exact column alignment specified in Murray [1988]. Horizontal spaces might have been inserted or left out from the following lists to improve their readability.

B.1 Sharp Cone (Air - Frozen Chemistry)

```
==> SHOT 671 FROZEN CHEMISTRY
$GR01
  KRI(1)=1,0,5,0,0,2,3,0,2,2,0,2,0,2,0,0,0,0,0,0,0,0,
  IDENT=0,
  IDRAG=0,
$END
$GR02
  NSP=1,
  NS=25,
$END
$GR03
  NTIME=1,
  IDISC(1)=1,1,1,1,1,1,1,1,1,1,1,1,1,1,1,
  TIME=-1.0,
  S(1)= 0.6,0.7,0.8,0.9,1.0,1.1,1.2,1.3,1.4,1.5,1.6,1.7,1.8,1.9,
        2.0,2.1,2.2,2.3,2.4,2.5,2.6,2.7,2.8,2.9,3.0
$END
$GR04
  NETA=15,
  ETA(1)= 0.0, 0.0005, 0.002, 0.01, 0.04, 0.072, 0.12, 0.20,
          0.32, 0.48, 0.80, 1.4, 2.0, 3.2, 5.0,
  KAPPA=13,
  CBAR=0.95,
$END
$GR05
  ROKAP(1)=-5.0,
$END
$GR07
  PTET(1)=237.67,
  GE(1)=9128.76,
  RADFL(1)=0.0,
$END
$GR08
  ELCON=0.4, YAP=-11.8, CLNUM=0.0168, SCT=0.9, PRT=-0.44, RETR=1000,
$END
$GR09
  GW=2000.0,
$END
$GR10
  PRDUM=0.7089,
  VMUA=7.3094E-07, VMUB=1.5, VMUC=1.0, VMUD=198.6,
  NC=5,
$END
```

```
N                    14.0080 0.000113 1 2
112964.   13441.2 4.92461 .0000271 9560.39 48.0916  500.  2500.  N
112964.   13427.7 2.77722 .0005234 5677290 48.0868 2500.  6000.  N
O                    15.9994 0.206210 1 2
59558.9 13516.6 4.96176 .0000057 29868.0  50.0932  500.  2500.  O
59558.9 13521.0 4.50112 .0001339 904980.  50.0947 2500.  6000.  O
NO                   30.0061 0.036495 1 2
21579.9 22750.8 8.08175 .0003545 -276336.  68.8669  500.  2500.  NO
21579.9 22714.5 8.77301 .0000727 -192889.  68.8541 2500.  6000.  NO
O2                   31.9988 0.068582 1 2
.574000 23444.1 8.07265 .0005031 -238837.  67.9715  500.  2500.  O2
.574000 23455.4 9.77777 .0001106 -4763670  67.9755 2500.  6000.  O2
N2                   28.0134 0.688700 1 2
-.110 22236.8 7.60394 .0005015 -234708.  63.7903  500.  2500.  N2
-.110 22184.2 8.58948 .0000972 -78141.1  63.7717 2500.  6000.  N2
$GR15
  PRE(1)= 0.0025756,0.0025756,0.0025756,0.0025756,0.0025756,0.0025756,
          0.0025756,0.0025756,0.0025756,0.0025756,0.0025756,0.0025756,
          0.0025756,0.0025756,0.0025756,0.0025756,0.0025756,0.0025756,
          0.0025756,0.0025756,0.0025756,0.0025756,0.0025756,0.0025756,
          0.0025756,
$END
$GR16
  TW = 541.0, 541.0, 541.0, 541.0, 541.0, 541.0, 541.0, 541.0, 541.0,
       541.0, 541.0, 541.0, 541.0, 541.0, 541.0, 541.0, 541.0, 541.0,
       541.0, 541.0, 541.0, 541.0, 541.0, 541.0, 541.0,
$END
```

B.2 Sharp Cone (Air - Nonequilibrium Chemistry/Catalytic Wall)

```
==> SHOT 671 NONEQUILIBRIUM CHEMISTRY - CATALYTIC WALL
$GR01
  KRI(1)=1,0,5,0,0,2,2,0,2,0,0,8,0,0,0,0,0,0,0,0,0,0,
  IDENT=0,
  IDRAG=0,
$END
$GR02
  NSP=5,
  NS=25,
$END
$GR03
  NTIME=1,
  IDISC(1)=0,0,0,0,0,0,0,0,0,0,0,0,0,0,0,0,0,
  TIME=-1.0,
  S(1)= 0.6,0.7,0.8,0.9,1.0,1.1,1.2,1.3,1.4,1.5,1.6,1.7,1.8,1.9,
        2.0,2.1,2.2,2.3,2.4,2.5,2.6,2.7,2.8,2.9,3.0,
$END
$GR04
  NETA=15,
  ETA(1)= 0.0, 0.0005, 0.002, 0.01, 0.04, 0.072, 0.12, 0.20,
          0.32, 0.48, 0.80, 1.4, 2.0, 3.2, 5.0,
  KAPPA=13,
  CBAR=0.95,
$END
$GR05
 ROKAP(1)=-5.0,
$END
$GR07
 PTET(1)=237.67,
 GE(1)=9128.76,
 RADFL(1)=0.0,
$END
$GR08
 ELCON=0.40, YAP=-11.8, CLNUM=0.0168, SCT=0.9, PRT=-0.44, RETR=1000,
$END
$GR09
 GW=150.0,
 SPFG(1)=0.00133, 0.00214, 0.0029, 0.20,
$END
  5
  7NITROGEN 14.008 .0001128
  8OXYGEN   16.0   .2062100
```

```
11NI-OXIDE  30.008 .0364950
10OXYGEN2   32.0   .0685820
 9NITROGEN2 28.016 .6887000
1 7 0 0 0 0 0 0 0 0 0 0 0 0 0JANAF TAPE 7/71 3/61                          N
112964+6 134412+5 492461+1 271364-4 956039+4 480916+2  500.  2500.1 -0.N
112964+6 134277+5 277722+1 523356-3 567729+7 480868+2 2500.  6000.1 -0.N
1 8 0 0 0 0 0 0 0 0 0 0 0 0 0JANAF TAPE 7/71 6/62                         O
595589+5 135166+5 496176+1 567346-5 298680+5 500932+2  500.  2500.1 -0.O
595589+5 135210+5 450112+1 133922-3 904980+6 500947+2 2500.  6000.1 -0.O
1 11 0 0 0 0 0 0 0 0 0JANAF TAPE 7/71 6/63                              NO
215799+5 227508+5 808175+1 354495-3-276336+6 688669+2  500.  2500.1 -0.NO
215799+5 227145+5 877301+1 726516-4-192889+6 688541+2 2500.  6000.1 -0.NO
1 10 0 0 0 0 0 0 0 0 0 0 0 0 0JANAF TAPE 7/71 **/61                       O2
574000+0 234441+5 807265+1 503078-3-238837+6 679715+2  500.  2500.1 -0.O2
574000+0 234554+5 977777+1 110622-3-476367+7 679755+2 2500.  6000.1 -0.O2
1 9 0 0 0 0 0 0 0 0 0 0 0 0 0JANAF TAPE 7/71 **/61                        N2
-110 0+0 222368+5 760394+1 501467-3-234708+6 637903+2  500.  2500.1 -0.N2
-110 0+0 221842+5 858948+1 972320-4-781411+5 637717+2 2500.  6000.1 -0.N2

3 6 0
                1.0 O == .5 O2
1.0E+6 0.0 0.0
                1.0 N == .5 N2
1.0E+6 0.0 0.0
                1.0 NO == .5 O2 .5 N2
1.0E+6 0.0 0.0
                1.0 THBD 1.0 O2 == 2.0 O
N NO O O2 N2
3.61 3.61 90.25 32.5 7.22
1.00E18 -1.0 59400.0 0.0
                1.0 THBD 1.0 N2 == 2.0 N
O O2 NO N2
1.92 1.92 1.92 4.80
1.00E17 -0.5 113100.0 0.0
                1.0 N2 1.0 N == 3.0 N
4.15E22 -1.5 113100.0 0.0
                1.0 THBD 1.0 NO == 1.0 N 1.0 O
O2 N2 N O NO
3.97 3.97 79.4 79.4 79.4
1.00E20 -1.5 76500.0 0.0
                1.0 NO 1.0 O == 1.0 O2 1.0 N
3.18E09 1.0 19700.0 0.0
                1.0 N2 1.0 O == 1.0 NO 1.0 N
6.75E13 0.0 37500.0 0.0
```

```
$GR15
 PRE(1)= 0.0025756,0.0025756,0.0025756,0.0025756,0.0025756,0.0025756,
         0.0025756,0.0025756,0.0025756,0.0025756,0.0025756,0.0025756,
         0.0025756,0.0025756,0.0025756,0.0025756,0.0025756,0.0025756,
         0.0025756,0.0025756,0.0025756,0.0025756,0.0025756,0.0025756,
         0.0025756,
 SPECE(1,1)= .0001128,.0001128,.0001128,.0001128,.0001128,.0001128,
             .0001128,.0001128,.0001128,.0001128,.0001128,.0001128,
             .0001128,.0001128,.0001128,.0001128,.0001128,.0001128,
             .0001128,.0001128,.0001128,.0001128,.0001128,.0001128,
             .0001128,
 SPECE(1,2)= .2062100,.2062100,.2062100,.2062100,.2062100,.2062100,
             .2062100,.2062100,.2062100,.2062100,.2062100,.2062100,
             .2062100,.2062100,.2062100,.2062100,.2062100,.2062100,
             .2062100,.2062100,.2062100,.2062100,.2062100,.2062100,
             .2062100,
 SPECE(1,3)= .0364950,.0364950,.0364950,.0364950,.0364950,.0364950,
             .0364950,.0364950,.0364950,.0364950,.0364950,.0364950,
             .0364950,.0364950,.0364950,.0364950,.0364950,.0364950,
             .0364950,.0364950,.0364950,.0364950,.0364950,.0364950,
             .0364950,
 SPECE(1,4)= .0685820,.0685820,.0685820,.0685820,.0685820,.0685820,
             .0685820,.0685820,.0685820,.0685820,.0685820,.0685820,
             .0685820,.0685820,.0685820,.0685820,.0685820,.0685820,
             .0685820,.0685820,.0685820,.0685820,.0685820,.0685820,
             .0685820,
 SPECE(1,5)= .6887000,.6887000,.6887000,.6887000,.6887000,.6887000,
             .6887000,.6887000,.6887000,.6887000,.6887000,.6887000,
             .6887000,.6887000,.6887000,.6887000,.6887000,.6887000,
             .6887000,.6887000,.6887000,.6887000,.6887000,.6887000,
             .6887000,
$END
$GR16
 TW = 541.0, 541.0, 541.0, 541.0, 541.0, 541.0, 541.0, 541.0, 541.0,
      541.0, 541.0, 541.0, 541.0, 541.0, 541.0, 541.0, 541.0, 541.0,
      541.0, 541.0, 541.0, 541.0, 541.0, 541.0, 541.0,
$END
```

B.3 Sharp Cone (CO_2 - Frozen Chemistry)

```
==> SHOT 1144 FROZEN CHEMISTRY
$GR01
  KRI(1)=1,0,5,0,0,2,3,0,2,2,0,2,0,2,0,0,0,0,0,0,0,0,
  IDENT=0,
  IDRAG=0,
$END
$GR02
  NSP=1,
  NS=25,
$END
$GR03
  NTIME=1,
  IDISC(1)=1,1,1,1,1,1,1,1,1,1,1,1,1,1,1,
  TIME=-1.0,
  S(1)= 0.6,0.7,0.8,0.9,1.0,1.1,1.2,1.3,1.4,1.5,1.6,1.7,1.8,1.9,
        2.0,2.1,2.2,2.3,2.4,2.5,2.6,2.7,2.8,2.9,3.0
$END
$GR04
  NETA=15,
  ETA(1)= 0.0, 0.0005, 0.002, 0.01, 0.04, 0.072, 0.12, 0.20,
          0.32, 0.48, 0.80, 1.4, 2.0, 3.2, 5.0,
  KAPPA=13,
  CBAR=0.95,
$END
$GR05
  ROKAP(1)=-5.0,
$END
$GR07
  PTET(1)=1931.51,
  GE(1)=63.52,
  RADFL(1)=0.0,
$END
$GR08
  ELCON=0.4, YAP=-11.8, CLNUM=0.0168, SCT=0.9, PRT=-0.44, RETR=10000,
$END
$GR09
  GW=2000.0,
$END
$GR10
  PRDUM=0.833,
  VMUA=7.80833E-07, VMUB=1.5, VMUC=1.0, VMUD=435.642,
  NC=5,
$END
```

```
O                    15.9994 0.006080 1 2
59511.   13235.   4.929 0.0 0.0 50.093  500.   3000.1 0.O
59511.   13235.   4.929 0.0 0.0 50.093 3000.   5000.1 0.O
C                    12.0110 0.000000 1 2
171165.   12827.   4.802 0.0 0.0 49.288  500.   3000.1 0.C
171165.   12827.   4.802 0.0 0.0 49.288 3000.   5000.1 0.C
CO                   28.0104 0.153126 1 2
-26398.   21532.   8.541 0.0 0.0 65.294  500.   3000.1 0.CO
-26398.   21532.   8.541 0.0 0.0 65.294 3000.   5000.1 0.CO
O2                   31.9988 0.073525 1 2
21521.   8.355 0.0 0.0 67.910  500.   3000.1 0.O2
21521.   8.355 0.0 0.0 67.910 3000.   5000.1 0.O2
CO2                  44.0098 0.767268 1 2
-93987.   34974.   14.26 0.0 0.0 79.696  500.   3000.1 0.CO2
-93987.   34974.   14.26 0.0 0.0 79.696 3000.   5000.1 0.CO2
$GR15
  PRE(1)= .0004287,.0004287,.0004287,.0004287,.0004287,.0004287,
          .0004287,.0004287,.0004287,.0004287,.0004287,.0004287,
          .0004287,.0004287,.0004287,.0004287,.0004287,.0004287,
          .0004287,.0004287,.0004287,.0004287,.0004287,.0004287,
          .0004287,
$END
$GR16
  TW = 541.0, 541.0, 541.0, 541.0, 541.0, 541.0, 541.0, 541.0, 541.0,
       541.0, 541.0, 541.0, 541.0, 541.0, 541.0, 541.0, 541.0, 541.0,
       541.0, 541.0, 541.0, 541.0, 541.0, 541.0, 541.0,
$END
```

B.4 Sharp Cone (CO_2 - Nonequilibrium Chemistry/Catalytic Wall)

```
==> SHOT 1144 NONEQUILIBRIUM CHEMISTRY - CATALYTIC WALL
$GR01
  KRI(1)=1,0,5,0,0,2,2,0,2,0,0,8,0,0,0,0,0,0,0,0,0,0,
  IDENT=0,
  IDRAG=0,
$END
$GR02
  NSP=5,
  NS=25,
$END
$GR03
  NTIME=1,
  IDISC(1)=0,0,0,0,0,0,0,0,0,0,0,0,0,0,0,0,0,0,0,0,0,
  TIME=-1.0,
  S(1)= 0.6,0.7,0.8,0.9,1.0,1.1,1.2,1.3,1.4,1.5,1.6,1.7,1.8,1.9,
        2.0,2.1,2.2,2.3,2.4,2.5,2.6,2.7,2.8,2.9,3.0,
$END
$GR04
  NETA=15,
  ETA(1)= 0.0, 0.0005, 0.002, 0.01, 0.04, 0.072, 0.12, 0.20,
          0.32, 0.48, 0.80, 1.4, 2.0, 3.2, 5.0,
  KAPPA=13,
  CBAR=0.95,
$END
$GR05
 ROKAP(1)=-5.0,
$END
$GR07
 PTET(1)=1931.51,
 GE(1)=63.52,
 RADFL(1)=0.0,
$END
$GR08
 ELCON=0.40, YAP=-11.8, CLNUM=0.0168, SCT=0.9, PRT=-0.44, RETR=10000,
$END
$GR09
 GW=2200.0,
 SPFG(1)=0.0000001,0.0000001,0.1100,0.066700,
$END
  5
  8OXYGEN  16.0   0.006080
  6CARBON  12.011 0.000000
```

```
11CARB-MONOX  28.011 0.153126
10OXYGEN2     32.0   0.073525
 9CARB-DIOX   44.011 0.767268
1 8 0 0 0 0 0 0 0 0 0 0 0 0 0JANAF TAPE 7/71 6/62                          0
595589+5 135166+5 496176+1 567346-5 298680+5 500932+2  500.  2500.1 -0.0
595589+5 135210+5 450112+1 133922-3 904980+6 500947+2 2500.  6000.1 -0.0
1 6 0 0 0 0 0 0 0 0 0 0 0 0 0JANAF TAPE 7/71 3/61                          C
170885+6 135249+5 486179+1 753554-4 220874+5 492786+2  500.  2500.1 -0.C
170885+6 135492+5 514716+1 766698-4-178199+7 492872+2 2500.  6000.1 -0.C
1 11 0 0 -0 -0 -0 -0 -0 -0 -0 -0 -0 -0JANAF TAPE 7/71 3/61              CO
-264169+5 224202+5 779944+1 441449-3-262021+6 653923+2  500.  2500.1 -0.CO
-264169+5 223744+5 866947+1 865971-4-155174+6 653761+2 2500.  6000.1 -0.CO
1 10 0 0 0 0 0 0 0 0 0 0 0 0 0JANAF TAPE 7/71 **/61                        02
574000+0 234441+5 807265+1 503078-3-238837+6 679715+2  500.  2500.1 -0.02
574000+0 234554+5 977777+1 110622-3-476367+7 679755+2 2500.  6000.1 -0.02
1 9 0 0 0 0 0 0 0 0 0 0 0 0 0JANAF TAPE 7/71 3/61                         CO2
-940539+5 366362+5 130735+2 733664-3-754525+6 798849+2  500.  2500.1 -0.CO2
-940539+5 365610+5 142661+2 209831-3-233974+5 798583+2 2500.  6000.1 -0.CO2

2 6 0
               1.0 O == .5 O2
1.0E+6 0.0 0.0
               1.0 CO 1.0 O == 1.0 CO2
1.0E+6 0.0 0.0
               1.0 THBD 1.0 O2 == 2.0 O
O C CO O2 CO2
10.0 10.0 2.00 2.00 2.00
1.00E21 -1.5 59750.0 0.0
               1.0 THBD 1.0 CO2 == 1.0 CO 1.0 O
O C CO O2 CO2
1.00 1.00 1.00 1.00 1.00
3.70E14 -0.0 52500.0 0.0
               1.0 THBD 1.0 CO == 1.0 C 1.0 O
O C CO O2 CO2
34.0 34.0 4.48 2.30 2.30
1.00E19 -1.0 129000.  0.0
               1.0 CO2 1.0 O == 1.0 CO 1.0 O2
1.70E13 0.0 26500.0 0.0
               1.0 CO 1.0 O == 1.0 C 1.0 O2
3.90E13 -.18 69200.0 0.0
               1.0 CO 1.0 CO == 1.0 CO2 1.0 C
2.33E9 0.5 65710.0 0.0
```

```
$GR15
 PRE(1)= .0004287,.0004287,.0004287,.0004287,.0004287,.0004287,
         .0004287,.0004287,.0004287,.0004287,.0004287,.0004287,
         .0004287,.0004287,.0004287,.0004287,.0004287,.0004287,
         .0004287,.0004287,.0004287,.0004287,.0004287,.0004287,
         .0004287,
 SPECE(1,1)= .006080,.006080,.006080,.006080,.006080,.006080,
             .006080,.006080,.006080,.006080,.006080,.006080,
             .006080,.006080,.006080,.006080,.006080,.006080,
             .006080,.006080,.006080,.006080,.006080,.006080,
             .006080,
 SPECE(1,2)= .000000,.000000,.000000,.000000,.000000,.000000,
             .000000,.000000,.000000,.000000,.000000,.000000,
             .000000,.000000,.000000,.000000,.000000,.000000,
             .000000,.000000,.000000,.000000,.000000,.000000,
             .000000,
 SPECE(1,3)= .153126,.153126,.153126,.153126,.153126,.153126,
             .153126,.153126,.153126,.153126,.153126,.153126,
             .153126,.153126,.153126,.153126,.153126,.153126,
             .153126,.153126,.153126,.153126,.153126,.153126,
             .153126,
 SPECE(1,4)= .073525,.073525,.073525,.073525,.073525,.073525,
             .073525,.073525,.073525,.073525,.073525,.073525,
             .073525,.073525,.073525,.073525,.073525,.073525,
             .073525,.073525,.073525,.073525,.073525,.073525,
             .073525,
 SPECE(1,5)= .767268,.767268,.767268,.767268,.767268,.767268,
             .767268,.767268,.767268,.767268,.767268,.767268,
             .767268,.767268,.767268,.767268,.767268,.767268,
             .767268,.767268,.767268,.767268,.767268,.767268,
             .767268,
$END
$GR16
 TW = 541.0, 541.0, 541.0, 541.0, 541.0, 541.0, 541.0, 541.0, 541.0,
      541.0, 541.0, 541.0, 541.0, 541.0, 541.0, 541.0, 541.0, 541.0,
      541.0, 541.0, 541.0, 541.0, 541.0, 541.0, 541.0,
$END
```